

# Hyperbolic Geometry, Nehari's Theorem, Electric Circuits, and Analog Signal Processing

JEFFERY C. ALLEN AND DENNIS M. HEALY, JR.

ABSTRACT. Underlying many of the current mathematical opportunities in digital signal processing are unsolved analog signal processing problems. For instance, digital signals for communication or sensing must map into an analog format for transmission through a physical layer. In this layer we meet a canonical example of analog signal processing: the electrical engineer's *impedance matching problem*. Impedance matching is the design of analog signal processing circuits to minimize loss and distortion as the signal moves from its source into the propagation medium. This paper works the matching problem from theory to sampled data, exploiting links between  $H^\infty$  theory, hyperbolic geometry, and matching circuits. We apply J. W. Helton's significant extensions of operator theory, convex analysis, and optimization theory to demonstrate new approaches and research opportunities in this fundamental problem.

## CONTENTS

|  |    |
|--|----|
| 1. The Impedance Matching Problem        | 2  |
| 2. A Synopsis of the $H^\infty$ Solution | 4  |
| 3. Technical Preliminaries               | 8  |
| 4. Electric Circuits                     | 12 |
| 5. $H^\infty$ Matching Techniques        | 27 |
| 6. Classes of Lossless 2-Ports           | 35 |
| 7. Orbits and Tight Bounds for Matching  | 39 |
| 8. Matching an HF Antenna                | 42 |
| 9. Research Topics                       | 47 |
| 10. Epilogue                             | 52 |
| A. Matrix-Valued Factorizations          | 52 |
| B. Proof of Lemma 4.4                    | 55 |
| C. Proof of Theorem 6.1                  | 56 |
| D. Proof of Theorem 5.5                  | 56 |
| References                               | 59 |

---

Allen gratefully acknowledges support from ONR and the IAR Program at SCC San Diego. Healy was supported in part by ONR.

## 1. The Impedance Matching Problem

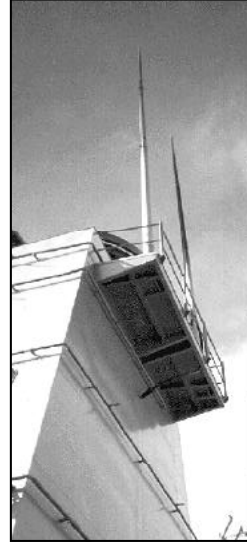
Figure 1 shows a twin-whip HF (high-frequency) antenna mounted on a superstructure representative of a shipboard environment. If a signal generator is connected directly to this antenna, not all the power delivered to the antenna can be radiated by the antenna. If an *impedance mismatch* exists between the signal generator and the antenna, some of the signal power is reflected from the antenna back to the generator. To effectively use this antenna, a *matching circuit* must be inserted between the signal generator and antenna to minimize this wasted power.

Figure 2 shows the matching circuit connecting the generator to the antenna. Port 1 is the input from the generator. Port 2 is the output that feeds the antenna.

The matching circuit is called a *2-port*. Because the 2-port must not waste power, the circuit designer only considers *lossless 2-ports*. The mathematician knows the lossless 2-ports as the  $2 \times 2$  inner functions. The matching problem is to find a lossless 2-port that transfers as much power as possible from the generator to the antenna.

The mathematical reader can see antennas everywhere: on cars, on rooftops, sticking out of cell phones. A realistic model of an antenna is extremely complex because the antenna is embedded in its environment. Fortunately, we only need to know how the antenna behaves as a 1-port device. As indicated in Figure 2, the antenna's *scattering function* or *reflectance*  $s_L$  characterizes its 1-port behavior. The mathematician knows  $s_L$  as an element in the unit ball of  $H^\infty$ .

Figure 3 displays  $s_L : j\mathbb{R} \rightarrow \mathbb{C}$  of an HF antenna measured over the frequency range of 9 to 30 MHz. (Here  $j = +\sqrt{-1}$  because  $i$  is used for current.) At each radian frequency  $\omega = 2\pi f$ , where  $f$  is the frequency in Hertz,  $s_L(j\omega)$  is a



Courtesy of Antenna Products

Figure 1

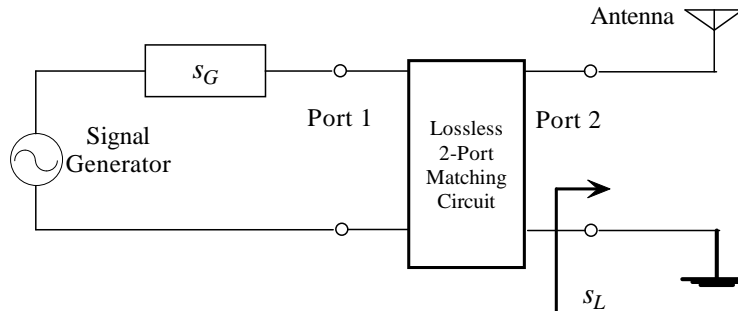
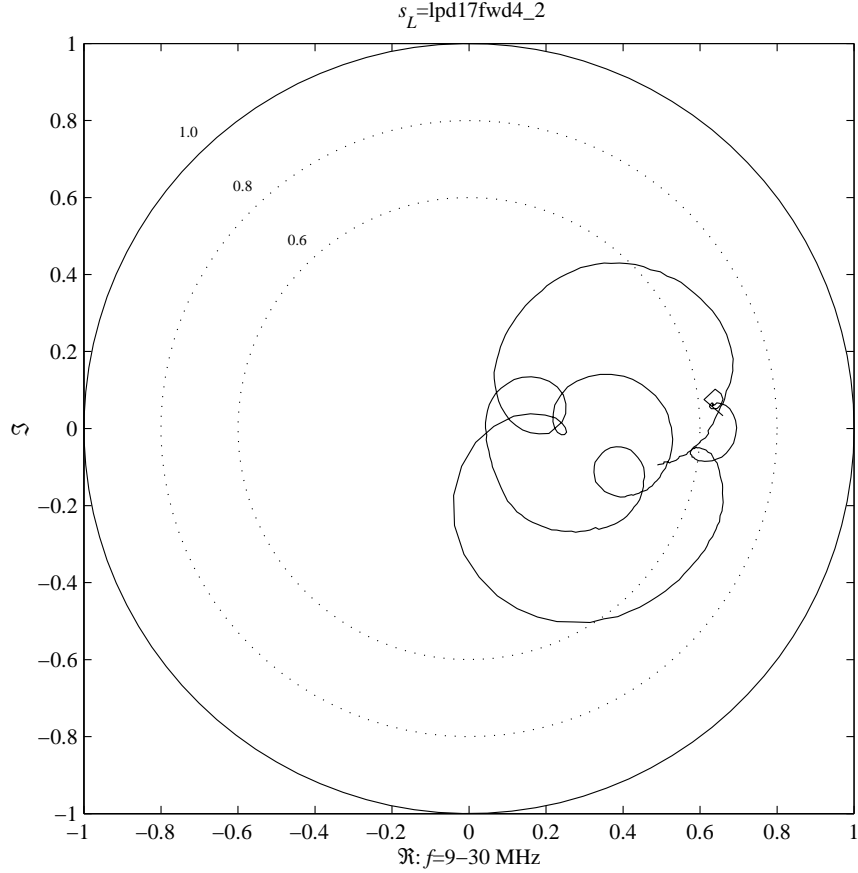


Figure 2. An antenna connected to a lossless matching 2-port.

complex number in the unit disk that specifies the relative strength and phase of the reflection from the antenna when it is driven by a pure tone of frequency  $\omega$ .  $s_L(j\omega)$  measures how efficiently we could broadcast a pure sinusoid of frequency  $\omega$  by directly connecting the sinusoidal signal generator to the antenna. If  $|s_L(j\omega)|$  is near 0, almost no signal is reflected back by the antenna towards



**Figure 3.** The reflectance  $s_L(j\omega)$  of an HF antenna.

the generator or, equivalently, almost all of the signal power passes through the antenna to be radiated into space. If  $|s_L(j\omega)|$  is near 1, most of this signal is reflected back from the antenna and so very little signal power is radiated.

Most signals are not pure tones, but may be represented in the usual way as a Fourier superposition of pure tones taken over a band of frequencies. In this case, the reflectance function evaluated at each frequency in the band multiplies the corresponding frequency component of the incident signal. The net reflection is the superposition of the resulting component reflections. To ensure that an undistorted version of the generated signal is radiated from the antenna,

the circuit designer looks for a lossless 2-port that “pulls  $s_L(j\omega)$  to 0 over all frequencies in the band.” As a general rule, the circuit designer must pull  $s_L$  inside the disk of radius 0.6 at the very least.

To take a concrete example, the circuit designer may match the HF antenna using a transformer as shown in Figure 4. If we put a signal into in Port 1

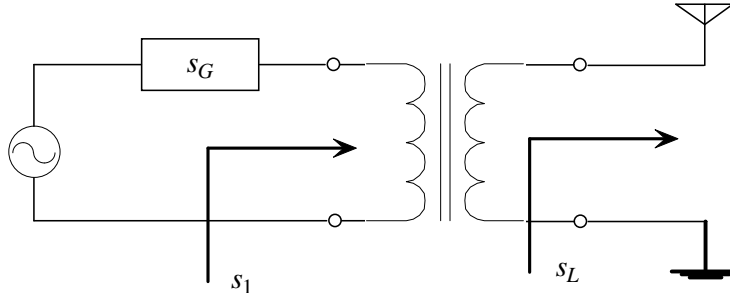


**Figure 4.** An antenna connected to a matching transformer.

of the transformer and measure the reflected signal, their ratio is the scattering function  $s_1$ . That is,  $s_1$  is how the antenna looks when viewed through the transformer. The circuit designer attempts to find a transformer so that the “matched antenna” has a small reflectance. Figure 5 shows the optimal transformer does provide a minimally acceptable match for the HF antenna. The grey disk shows all reflectances  $|s| \leq 0.6$  and contains  $s_1(j\omega)$  over the frequency band.

However, this example raises the following question: *Could we do better with a different matching circuit?* Typically, a circuit designer selects a circuit topology, selects the reactive elements (inductors and capacitors), and then undertakes a constrained optimization over the acceptable element values. The difficulty of this approach lies in the fact that there are many circuit topologies and each presents a highly nonlinear optimization problem. This forces the circuit designer to undertake a massive search to determine an optimal network topology with no stopping criteria. In practice, often the circuit designer throws circuit after circuit at the problem and hopes for a lucky hit. And there is always the nagging question: *What is the best matching possible?* Remarkably, “pure” mathematics has much to say about this analog signal processing problem.

## 2. A Synopsis of the $H^\infty$ Solution

Our presentation of the impedance matching problem weaves together many diverse mathematical and technological threads. This motivates beginning with the big picture of the story, leaving the details of the structure to the subsequent sections. In this spirit, the reader is asked to accept for now that to every  $N$ -port (generalizing the 1- and 2-ports we have just encountered), there

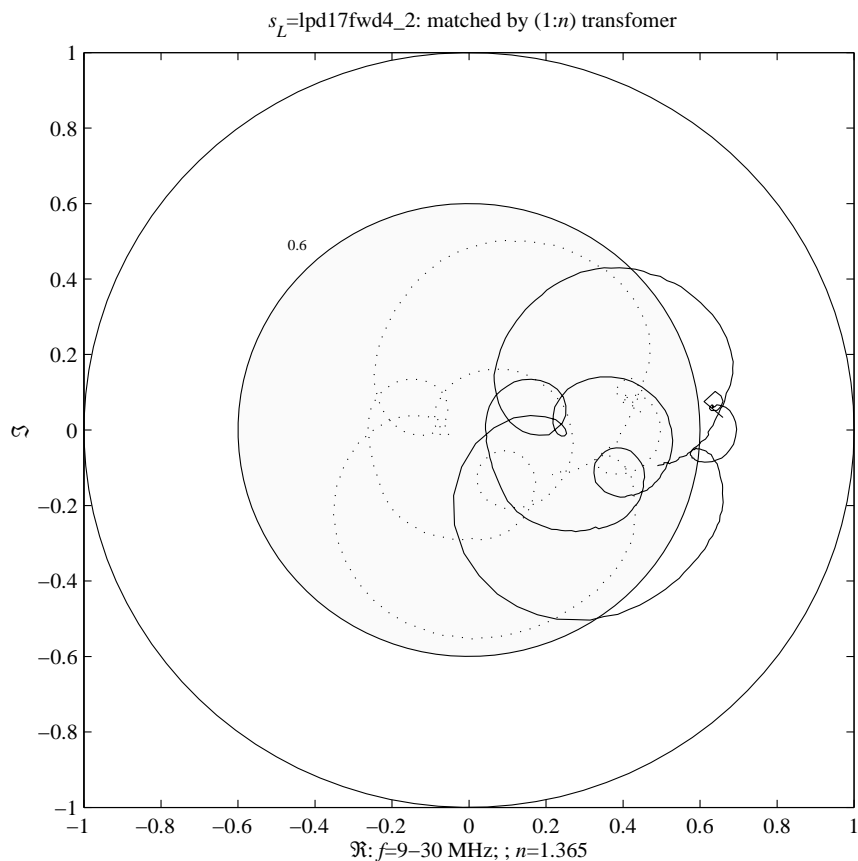


**Figure 5.** The reflectance  $s_L$  (solid line) of an HF antenna and the reflectance  $s_1$  (dotted line) obtained by a matching transformer.

corresponds an  $N \times N$  scattering matrix  $S \in H^\infty(\mathbb{C}_+, \mathbb{C}^{N \times N})$ , whose entries are analytic functions of frequency generalizing the reflectances of the previous section. Mathematically,  $S : \mathbb{C}_+ \rightarrow \mathbb{C}^{N \times N}$  is a mapping from open right half plane  $\mathbb{C}_+$  (parameterizing complex frequency) to the space of complex  $N \times N$  matrices that is analytic and bounded with sup-norm

$$\|S\|_\infty := \text{ess.sup}\{\|S(j\omega)\| : \omega \in \mathbb{R}\} < \infty.$$

For a 1-port,  $S$  is scalar-valued and, as we saw previously, is called a scattering function or *reflectance*. Scattering matrix entries for physical circuits are not arbitrary functions of frequency. The circuits in this paper are linear, causal, time-invariant, and solvable. These constraints force their scattering matrices into  $H^\infty$ ; see [3; 4; 31].

Figure 6 presents the schematic of the matching 2-port. The matching 2-port is characterized by its  $2 \times 2$  scattering matrix

$$S(j\omega) = \begin{bmatrix} S_{11}(j\omega) & S_{12}(j\omega) \\ S_{21}(j\omega) & S_{22}(j\omega) \end{bmatrix}.$$

The matrix entries measure the output response of the 2-port. For example,  $s_{22}$

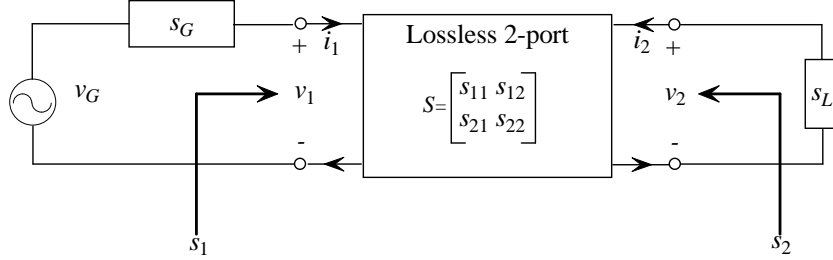


**Figure 6.** Matching circuit and reflectances.

measures the response reflected from Port 2 when a unit signal is driving Port 2;  $s_{12}$  is the signal from Port 1 in response to a unit signal input to Port 2. If the 2-port consumes power, it is called *passive* and its corresponding scattering matrix is a contraction on  $j\mathbb{R}$ :

$$S(j\omega)^H S(j\omega) \leq \begin{bmatrix} 1 & 0 \\ 0 & 1 \end{bmatrix}$$

almost everywhere in frequency (a.e. in  $\omega$ ), or equivalently that  $S$  belongs to the closed unit ball:  $S \in \bar{B}H^\infty(\mathbb{C}_+, \mathbb{C}^{2 \times 2})$ . The reflectances of the generator and load are assumed to be passive also:  $s_G, s_L \in \bar{B}H^\infty(\mathbb{C}_+)$ . Because the goal is to avoid wasting power, the circuit designer matches the generator to the load using a *lossless* 2-port:

$$S(j\omega)^H S(j\omega) = \begin{bmatrix} 1 & 0 \\ 0 & 1 \end{bmatrix} \quad \text{a.e.}$$

Scattering matrices satisfying this constraint provide the most general model for lossless 2-ports. These are the  $2 \times 2$  *real inner functions*, denoted by  $U^+(2) \subset H^\infty(\mathbb{C}_+, \mathbb{C}^{2 \times 2})$ . The circuit designer does not actually have access to all of  $U^+(2)$  through practical electrical networks. Instead, the circuit designer optimizes over a practical subclass  $\mathcal{U} \subset U^+(2)$ . For example, some antenna applications restrict the total number  $d$  of inductors and capacitors. In this case,  $\mathcal{U} = U^+(2, d)$  consists of the real, rational, inner functions of Smith–McMillan degree not exceeding degree  $d$  ( $d$  defined in Theorem 6.2).

The figure-of-merit for the matching problem of Figure 6 is the transducer power gain  $G_T$  defined as the ratio of the power delivered to the load to the

maximum power available from the generator [44, pages 606-608]:

$$G_T(s_G, S, s_L) := |s_{21}|^2 \frac{1 - |s_G|^2}{|1 - s_1 s_G|^2} \frac{1 - |s_L|^2}{|1 - s_{22} s_L|^2}, \quad (2-1)$$

where  $s_1$  is the reflectance seen looking into Port 1 of the matching circuit at the load  $s_L$  terminating Port 2. This is computed by acting on  $s_L$  by a linear-fractional transform parameterized by the matrix  $S$ :

$$s_1 = \mathcal{F}_1(S, s_L) := s_{11} + s_{12} s_L (1 - s_{22} s_L)^{-1} s_{21}. \quad (2-2)$$

Likewise, looking into Port 2 with Port 1 terminated in  $s_G$  gives the reflectance

$$s_2 = \mathcal{F}_2(S, s_G) := s_{22} + s_{21} s_G (1 - s_{11} s_G)^{-1} s_{12}. \quad (2-3)$$

The worst case performance of the matching circuit  $S$  is represented by the minimum of the gain over frequency:

$$\|G_T(s_G, S, s_L)\|_{-\infty} := \text{ess.inf}\{|G_T(s_G, S, s_L; j\omega)| : \omega \in \mathbb{R}\}.$$

In terms of this gain we can formulate the *Matching Problem*:

**MATCHING PROBLEM.** *Maximize the worst case of the transducer power gain  $G_T$  over a collection  $\mathcal{U} \subseteq U^+(2)$  of matching 2-ports:*

$$\sup\{\|G_T(s_G, S, s_L)\|_{-\infty} : S \in \mathcal{U}\}.$$

The current approach is to convert the 2-port matching problem to an equivalent 1-port problem and optimize over an orbit in the hyperbolic disk. Specifically, the transducer power gain can be written

$$G_T(s_G, S, s_L) = 1 - \Delta P(\mathcal{F}_2(S, s_G), s_L)^2 = 1 - \Delta P(s_G, \mathcal{F}_1(S, s_L))^2,$$

where the *power mismatch*

$$\Delta P(s_1, s_2) := \left| \frac{\bar{s}_1 - s_2}{1 - s_1 s_2} \right|$$

is the *pseudohyperbolic distance* between  $\bar{s}_1$  and  $s_2$ . The *orbit* of the generator's reflectance  $s_G$  under the action of  $\mathcal{U}$  is the set of reflectances

$$\mathcal{F}_2(\mathcal{U}, s_G) := \{\mathcal{F}_2(S, s_G) : S \in \mathcal{U}\} \subseteq \bar{B}H^\infty(\mathbb{C}_+).$$

Thus, the matching problem is equivalent to maximizing the transducer power gain over this orbit. The transducer power gain is bounded as follows:

$$\begin{aligned} \sup\{\|G_T(s_G, S, s_L)\|_{-\infty} : S \in \mathcal{U}\} &= 1 - \inf\{\|\Delta P(\mathcal{F}_2(S, s_G), s_L)\|_\infty^2 : S \in \mathcal{U}\} \\ &= 1 - \inf\{\|\Delta P(s_2, s_L)\|_\infty^2 : s_2 \in \mathcal{F}_2(\mathcal{U}, s_G)\} \\ &\leq 1 - \inf\{\|\Delta P(s_2, s_L)\|_\infty^2 : s_2 \in \bar{B}H^\infty(\mathbb{C}_+)\}. \end{aligned}$$

Expressing matching in terms of power mismatch in this way manifests the underlying hyperbolic geometry approximation problem. The reflectance of the

generator is transformed to various new reflectances in the hyperbolic disk under the action of the possible matching circuits. We look for the closest approach of this orbit to the load  $s_L$  with respect to the (pseudo) hyperbolic metric. The last bound is reducible to a matrix calculation by a hyperbolic version of Nehari's Theorem [42], a classic result relating analytic approximation to an operator norm calculation. The resulting Nehari bound gives the circuit designer an upper limit on the possible performance for any class  $\mathcal{U} \subseteq U^+(2)$  of matching circuits. For some classes, this bound is tight, telling the circuit designer that the benchmark is essentially obtainable with matching circuits from the specified class. For example, when  $\mathcal{U}$  is the class of all lumped lossless 2-ports (networks of discrete inductors and capacitors)

$$U^+(2, \infty) := \bigcup_{d \geq 0} U^+(2, d)$$

and  $s_G = 0$ , Darlington's Theorem establishes that

$$\begin{aligned} \sup\{\|G_T(s_G = 0, S, s_L)\|_{-\infty} : S \in U^+(2, \infty)\} \\ = 1 - \inf\{\|\Delta P(s_2, s_L)\|_{\infty}^2 : s_2 \in \bar{B}H^{\infty}(\mathbb{C}_+)\}, \end{aligned}$$

provided  $s_L$  is sufficiently smooth. In this case, the circuit designer knows that there are lumped, lossless 2-ports that get arbitrarily close to the Nehari bound. The limitation of this approach is the requirement that the generator reflectance  $s_G = 0$ , which is not always true. Thus, a good research topic is to relax this constraint, or to generalize Darlington's Theorem. Another limitation of the techniques described in this paper is that the Nehari methods produce only a bound—they do not supply the matching circuit. However, the techniques do compute the optimal  $s_2$ , leading to another excellent research topic—the “unitary dilation” of  $s_2$  to a scattering matrix with  $s_2 = s_{22}$ . That such substantial research topics naturally arise shows how an applied problem brings depth to mathematical investigations.

### 3. Technical Preliminaries

The real numbers are denoted by  $\mathbb{R}$ . The complex numbers are denoted by  $\mathbb{C}$ . The set of complex  $M \times N$  matrices is denoted by  $\mathbb{C}^{M \times N}$ .  $I_N$  and  $0_N$  denote the  $N \times N$  identity and zero matrices. Complex frequency is written  $p = \sigma + j\omega$ . The open right-half plane is denoted by  $\mathbb{C}_+ := \{p \in \mathbb{C} : \operatorname{Re}[p] > 0\}$ . The open unit disk is denoted by  $\mathbf{D}$  and the unit circle by  $\mathbf{T}$ .

#### 3.1. Function spaces.

- $L^{\infty}(j\mathbb{R})$  denotes the class of Lebesgue-measurable functions defined on  $j\mathbb{R}$  with norm  $\|\phi\|_{\infty} := \operatorname{ess.\,sup}\{|\phi(j\omega)| : \omega \in \mathbb{R}\}$ .
- $C_0(j\mathbb{R})$  denotes the subspace of those continuous functions on  $j\mathbb{R}$  that vanish at  $\pm\infty$  with sup norm.

- $H^\infty(\mathbb{C}_+)$  denotes the Hardy space of functions bounded and analytic on  $\mathbb{C}_+$  with norm  $\|h\|_\infty := \sup\{|h(p)| : p \in \mathbb{C}_+\}$ .

$H^\infty(\mathbb{C}_+)$  is identified with a subspace of  $L^\infty(j\mathbb{R})$  whose elements are obtained by the pointwise limit  $h(j\omega) = \lim_{\sigma \rightarrow 0} h(\sigma + j\omega)$  that converges almost everywhere [39, page 153]. Convergence in norm occurs if and only if the  $H^\infty$  function has continuous boundary values. Those  $H^\infty$  functions with continuous boundary values constitute the *disk algebra*:

- $\mathcal{A}_1(\mathbb{C}_+) := 1 \dot{+} H^\infty(\mathbb{C}_+) \cap C_0(j\mathbb{R})$  denotes those continuous  $H^\infty(\mathbb{C}_+)$  functions that are constant at infinity.

These spaces nest as

$$\mathcal{A}_1(\mathbb{C}_+) \subset H^\infty(\mathbb{C}_+) \subset L^\infty(j\mathbb{R}).$$

Tensoring with  $\mathbb{C}^{M \times N}$  gives the corresponding matrix-valued functions:

$$L^\infty(j\mathbb{R}, \mathbb{C}^{M \times N}) := L^\infty(j\mathbb{R}) \otimes \mathbb{C}^{M \times N}$$

with norm  $\|\phi\|_\infty := \text{ess.sup}\{\|\phi(j\omega)\| : \omega \in \mathbb{R}\}$  induced by the matrix norm.

**3.2. The unit balls.** The *open unit ball* of  $L^\infty(j\mathbb{R}, \mathbb{C}^{M \times N})$  is denoted as

$$BL^\infty(j\mathbb{R}, \mathbb{C}^{M \times N}) := \left\{ \phi \in L^\infty(j\mathbb{R}, \mathbb{C}^{M \times N}) : \|\phi\|_\infty < 1 \right\}.$$

The *closed unit ball* of  $L^\infty(j\mathbb{R}, \mathbb{C}^{M \times N})$  is denoted as

$$\bar{B}L^\infty(j\mathbb{R}, \mathbb{C}^{M \times N}) := \left\{ \phi \in L^\infty(j\mathbb{R}, \mathbb{C}^{M \times N}) : \|\phi\|_\infty \leq 1 \right\}.$$

Likewise, the open unit ball of  $H^\infty(\mathbb{C}_+, \mathbb{C}^{M \times N})$  is

$$BH^\infty(\mathbb{C}_+, \mathbb{C}^{M \times N}) := BL^\infty(j\mathbb{R}, \mathbb{C}^{M \times N}) \cap H^\infty(\mathbb{C}_+, \mathbb{C}^{M \times N}).$$

**3.3. The real inner functions.** The class of *real*  $H^\infty(\mathbb{C}_+, \mathbb{C}^{M \times N})$  functions is denoted

$$\text{Re } H^\infty(\mathbb{C}_+, \mathbb{C}^{M \times N}) = \{S \in H^\infty(\mathbb{C}_+, \mathbb{C}^{M \times N}) : \overline{S(\bar{p})} = S(p)\}.$$

A function  $S \in H^\infty(\mathbb{C}_+, \mathbb{C}^{M \times N})$  is called *inner* provided

$$S(j\omega)^H S(j\omega) = I_N \quad \text{a.e.}$$

The class of *real inner* functions is denoted

$$U^+(N) := \{S \in \text{Re } \bar{B}H^\infty(\mathbb{C}_+, \mathbb{C}^{N \times N}) : S(j\omega)^H S(j\omega) = I_N \quad \text{a.e.}\}.$$

LEMMA 3.1.  $U^+(N)$  is closed subset of the boundary of  $\text{Re } \bar{B}H^\infty(\mathbb{C}_+, \mathbb{C}^{N \times N})$ .

PROOF. It suffices to show closure. If  $\{S_m\} \subset U^+(N)$  converges to  $S \in H^\infty(\mathbb{C}_+, \mathbb{C}^{N \times N})$ , then  $S_m(j\omega) \rightarrow S(j\omega)$  almost everywhere so that

$$I_N = \lim_{m \rightarrow \infty} S_m(j\omega)^H S_m(j\omega) = S(j\omega)^H S(j\omega) \quad \text{a.e.}$$

That is,  $S(j\omega)$  is unitary almost everywhere or  $S \in U^+(N)$ .  $\square$

**3.4. The weak-\* topology.** We use the weak-\* topology on  $L^\infty(j\mathbb{R}) = L^1(j\mathbb{R})^*$ . A weak-\* subbasis at  $0 \in L^\infty(j\mathbb{R})$  is the collection of weak-\* open sets

$$O[w, \varepsilon] := \{\phi \in L^\infty(j\mathbb{R}) : |\langle w, \phi \rangle| < \varepsilon\},$$

where  $\varepsilon > 0$ ,  $w \in L^1(j\mathbb{R})$ , and

$$\langle w, \phi \rangle := \int_{-\infty}^{\infty} w(j\omega)\phi(j\omega)d\omega.$$

Every weak-\* open set that contains  $0 \in L^\infty(j\mathbb{R})$  is a union of finite intersections of these subbasic sets. The Banach–Alaoglu Theorem [47, Theorem 3.15] gives that the unit ball  $\bar{B}L^\infty(j\mathbb{R})$  is weak-\* compact. The next lemma shows that the same holds for a distorted version of the unit ball, a fact that will have significant import for the optimization problems we consider later.

LEMMA 3.2. *Let  $c, r \in L^\infty(j\mathbb{R})$  with  $r \geq 0$  define the disk*

$$\bar{D}(c, r) := \{\phi \in L^\infty(j\mathbb{R}) : |\phi - c| \leq r \quad \text{a.e.}\}.$$

*Then  $\bar{D}(c, r)$  a closed, convex subset of  $L^\infty(j\mathbb{R})$  that is also weak-\* compact.*

PROOF. Closure and convexity follow from pointwise closure and convexity. To prove weak-\* compactness, let  $M_r : L^\infty(j\mathbb{R}) \rightarrow L^\infty(j\mathbb{R})$  be multiplication:  $M_r\phi := r\phi$ . Observe  $\bar{D}(k, r) = k + M_r\bar{B}L^\infty(j\mathbb{R})$ . Assume for now that  $M_r$  is weak-\* continuous. Then  $M_r\bar{B}L^\infty(j\mathbb{R})$  is weak-\* compact, because  $\bar{B}L^\infty(j\mathbb{R})$  is weak-\* compact, and the image of a compact set under a continuous function is compact. This forces  $\bar{D}(k, r)$  to be weak-\* compact, provided  $M_r$  is weak-\* continuous. To see that  $M_r$  is weak-\* continuous, it suffices to show that  $M_r$  pulls subbasic sets back to subbasic sets. Let  $\varepsilon > 0$ ,  $w \in L^1(j\mathbb{R})$ . Then

$$\begin{aligned} \psi \in M_r^{-1}(O[w, \varepsilon]) &\iff M_r\psi \in O[w, \varepsilon] \iff |\langle w, r\psi \rangle| < \varepsilon \\ &\iff |\langle rw, \psi \rangle| < \varepsilon \iff \psi \in O[rw, \varepsilon], \end{aligned}$$

noting that  $rw \in L^1(j\mathbb{R})$ .  $\square$

If  $K$  is a convex subset  $L^\infty(j\mathbb{R})$ , then  $K$  is closed  $\iff K$  is weak-\* closed [17, page 422]. Because  $H^\infty(\mathbb{C}_+)$  is a closed subspace of  $L^\infty(\mathbb{C}_+)$ , is it also weak-\* closed. Intersecting weak-\* closed  $H^\infty(\mathbb{C}_+)$  with the weak-\* compact unit ball of  $L^\infty(j\mathbb{R})$  forces  $\bar{B}H^\infty(\mathbb{C}_+)$  to be weak-\* compact.

**3.5. The Cayley transform.** Many computations are more conveniently placed in function spaces defined on the open unit disk  $\mathbf{D}$  rather than on the open right half-plane  $\mathbb{C}_+$ . The notation for the spaces on the disk follows the preceding nomenclature with the unit disk  $\mathbf{D}$  replacing  $\mathbb{C}_+$  and the unit circle  $\mathbf{T}$  replacing  $j\mathbb{R}$ .  $H^\infty(\mathbf{D})$  denotes the collection of analytic functions on the open unit disk with essentially bounded boundary values.  $C(\mathbf{T})$  denotes the continuous functions on the unit circle,  $\mathcal{A}(\mathbf{D}) := H^\infty(\mathbf{D}) \cap C(\mathbf{T})$  denotes the disk algebra, and  $L^\infty(\mathbf{T})$  denotes the Lebesgue-measurable functions on the unit circle  $\mathbf{T}$  with norm determined by the essential bound. A Cayley transform connects the function spaces on the right half plane to their counterparts on the disk.

LEMMA 3.3 ([27, page 99]). *Let the Cayley transform  $\mathbf{c} : \mathbb{C}_+ \rightarrow \mathbf{D}$*

$$\mathbf{c}(p) := \frac{p-1}{p+1}$$

*extend to the composition operator  $\mathbf{c} : L^\infty(\mathbf{T}) \rightarrow L^\infty(j\mathbb{R})$  as*

$$h(p) := H \circ \mathbf{c}(p) \quad (p = j\omega).$$

*Then  $\mathbf{c}$  is an isometry mapping*  $\left\{ \begin{array}{c} \mathcal{A}(\mathbf{D}) \\ H^\infty(\mathbf{D}) \\ C(\mathbf{T}) \\ L^\infty(\mathbf{T}) \end{array} \right\}$  *onto*  $\left\{ \begin{array}{c} \mathcal{A}_1(\mathbb{C}_+) \\ H^\infty(\mathbb{C}_+) \\ 1+C_0(j\mathbb{R}) \\ L^\infty(j\mathbb{R}) \end{array} \right\}$ .

**3.6. Factoring  $H^\infty$  functions.** The boundary values and *inner-outer* factorization of  $H^\infty$  functions are notions most conveniently developed on the unit disk and then transplanted to the right half-plane by the Cayley transform [35]. Let  $\phi \in L^1(\mathbf{T})$  have the Fourier expansion in  $z = \exp(j\theta)$

$$\phi(z) = \sum_{n=-\infty}^{\infty} \widehat{\phi}(n)z^n; \quad \widehat{\phi}(n) := \int_{-\pi}^{\pi} e^{-jn\theta} \phi(e^{j\theta}) \frac{d\theta}{2\pi}.$$

For  $1 \leq p \leq \infty$ , define  $H^p(\mathbf{D})$  as the subspace of  $L^p(\mathbf{T})$  with vanishing negative Fourier coefficients [27, page 77]:

$$H^p(\mathbf{D}) := \{h \in L^p(\mathbf{T}) : \widehat{h}(n) = 0 \text{ for } n = -1, -2, \dots\}.$$

Then  $H^p(\mathbf{D})$  is a closed subspace of  $L^p(\mathbf{T})$  and as [27, page 3]:

$$H^\infty(\mathbf{T}) \subset H^{p_2}(\mathbf{T}) \subset H^{p_1}(\mathbf{T}) \subset H^1(\mathbf{T}) \quad (1 \leq p_1 \leq p_2 \leq \infty)$$

Each  $h \in H^p(\mathbf{D})$  admits an analytic extension on the open unit disk [27, p. 77]:

$$h(z) = \sum_{n=0}^{\infty} \widehat{h}(n)z^n \quad (z = re^{j\theta}).$$

From the analytic extension, define  $h_r(e^{j\theta}) := h(re^{j\theta})$  for  $0 \leq r \leq 1$ . For  $r < 1$ ,  $h_r$  is continuous and analytic. As  $r$  increases to 1,  $h_r$  converges to  $h$  in the  $L^p$  norm, provided  $1 \leq p < \infty$ . For  $p = \infty$ ,  $h_r$  converges to  $h$  in the weak-\* topology

(discussed on page 10). If  $h_r$  does converge to  $h$  in the  $L^\infty$  norm, convergence is uniform and forces  $h \in \mathcal{A}(\mathbf{D})$ . Although disk algebra  $\mathcal{A}(\mathbf{D})$  is a strict subset of  $H^\infty(\mathbf{D})$  in the norm topology, it is a weak-\* dense subset.

If  $\phi$  is a positive, measurable function with  $\log(\phi) \in L^1(\mathbf{T})$  then the analytic function [48, page 370]:

$$q(z) = \exp \left( \int_{-\pi}^{\pi} \frac{e^{jt} + z}{e^{jt} - z} \log |\phi(e^{jt})| \frac{dt}{2\pi} \right) \quad (z \in \mathbf{D}),$$

is called an *outer function*. The magnitude of  $q(z)$  matches  $\phi$  [48, page 371]:

$$\lim_{r \rightarrow 1} |q_r(re^{j\theta})| = \phi(re^{j\theta}) \quad (\text{a.e.})$$

and leads to the equivalence:  $\phi \in L^p(\mathbf{T}) \iff q \in H^p(\mathbf{D})$ . We call  $q(z)$  a *spectral factor* of  $\phi$ . Every  $h \in H^\infty(\mathbf{D})$  admits an inner-outer factorization [48, pages 370-375]:

$$h(z) = e^{j\theta_0} b(z) s(z) q(z),$$

where the outer function  $q(z)$  is a spectral factor of  $|h|$  and the inner function consists of the *Blaschke product* [48, page 333]

$$b(z) := z^k \prod_{n=1}^{\infty} \frac{z_n - z}{1 - \bar{z}_n z} \frac{\bar{z}_n}{z_n},$$

$z_n \neq 0$ ,  $\sum(1 - |z_n|) < \infty$ , and the *singular inner function*

$$s(z) = \exp \left( - \int_{-\pi}^{\pi} \frac{e^{jt} + z}{e^{jt} - z} d\mu(t) \right),$$

for  $\mu$  a finite, positive, Borel measure on  $\mathbf{T}$  that is singular with respect to the Lebesgue measure. In the electrical engineering setup, we will see that the Blaschke products correspond to lumped, lossless circuits while a transmission line corresponds to a singular inner function.

#### 4. Electric Circuits

The impedance matching problem may be formulated as an optimization of certain natural figures of merit over structured sets of candidate electrical matching networks. We begin the formulation in this section, starting with an examination of the sorts of electrical networks available for impedance matching. Consideration of various choices of coordinate systems parameterizing the set of candidate matching circuits leads to the scattering formalism as the most suitable choice. Next we consider appropriate objective functions for measuring the utility of a candidate impedance matching circuit. This leads to description and characterization of power gain and mismatch functions as natural indicators of the suitability of our circuits. With the objective function and the parameterization of the admissible candidate set, we are in position to formulate impedance

matching as a constrained optimization problem. We will see that hyperbolic geometry plays a natural and enabling role in this formulation.

**4.1. Basic components.** Figure 7 represents an  $N$ -port—a box with  $N$  pairs of wire sticking out of it. The use of the word “port” means that each pair of wires obeys a *conservation of current*—the current flowing into one wire of the pair equals the current flowing out of the other wire. We can imagine

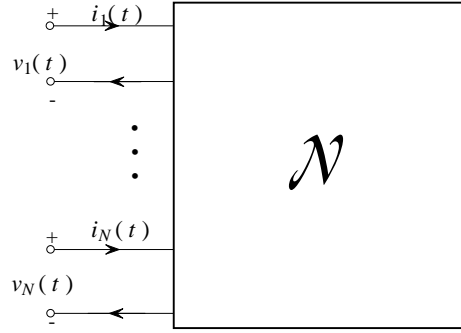


**Figure 7.** The  $N$ -port.

characterizing such a box by supplying current and voltage input signals of given frequency at the various ports and observing the current and voltages induced at the other ports. Mathematically, the  $N$ -port is defined as the collection  $\mathcal{N}$  of voltage  $\mathbf{v}(p)$  and current  $\mathbf{i}(p)$  vectors that can appear on its ports for all choices of the frequency  $p = \sigma + j\omega$  [31]:

$$\mathcal{N} \subseteq L^2(j\mathbb{R}, \mathbb{C}^N) \times L^2(j\mathbb{R}, \mathbb{C}^N).$$

If  $\mathcal{N}$  is a linear subspace, then the  $N$ -port is called a *linear*  $N$ -port. Figures 8 and 9 present the fundamental linear 1-ports and 2-ports. These examples show

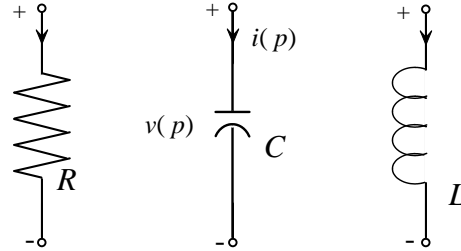


**Figure 8.** The lumped elements: resistor  $v(p) = Ri(p)$ ; capacitor  $i(p) = pCv(p)$ ; inductor  $v(p) = pLi(p)$ .

that  $\mathcal{N}$  can have the finer structure as the graph of a matrix-valued function: for instance, with the inductor  $\mathcal{N}$  is the graph of the function  $i(p) \mapsto pLi(p)$ .

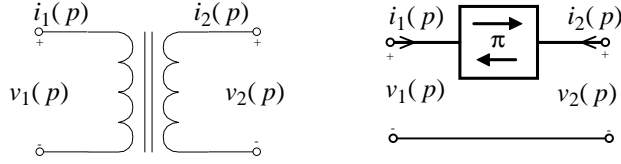


**Figure 9.** The transformer and gyrator.

More generally, if the voltage and current are related as  $\mathbf{v}(p) = Z(p)\mathbf{i}(p)$  then  $Z(p)$  is called the *impedance matrix* with real and imaginary parts  $Z(p) = R(p) + jX(p)$  called the resistance and reactance, respectively. If the voltage and current are related as  $\mathbf{i}(p) = Y(p)\mathbf{v}(p)$  then  $Y(p)$  is called the *admittance matrix* with real and imaginary parts  $Y(p) = B(p) + jG(p)$  called the conductance and susceptance, respectively. The *chain matrix*  $T(p)$  relates 2-port voltages and currents as

$$\begin{bmatrix} v_1 \\ i_1 \end{bmatrix} = \begin{bmatrix} t_{11}(p) & t_{12}(p) \\ t_{21}(p) & t_{22}(p) \end{bmatrix} \begin{bmatrix} v_2 \\ -i_2 \end{bmatrix}.$$

The ideal transformer has chain matrix [3, Eq. 2.4]:

$$\begin{bmatrix} v_1 \\ i_1 \end{bmatrix} = \begin{bmatrix} n^{-1} & 0 \\ 0 & n \end{bmatrix} \begin{bmatrix} v_2 \\ -i_2 \end{bmatrix}, \quad (4-1)$$

where  $n$  is the *turns ratio* of the windings on the transformer. The gyrator has chain matrix [3, Eq. 2.14]:

$$\begin{bmatrix} v_1 \\ i_1 \end{bmatrix} = \begin{bmatrix} 0 & \alpha \\ \alpha^{-1} & 0 \end{bmatrix} \begin{bmatrix} v_2 \\ -i_2 \end{bmatrix}.$$

Figure 10 shows how the 1-ports can build the series and shunt 2-ports with chain matrices

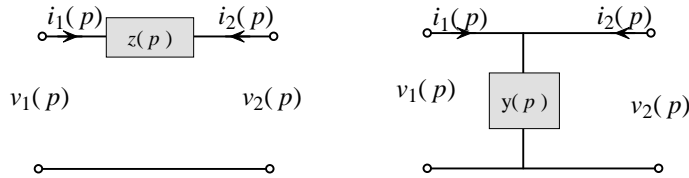


**Figure 10.** Series and shunt 2-ports.

$$T_{\text{series}}(p) = \begin{bmatrix} 1 & z(p) \\ 0 & 1 \end{bmatrix} \quad T_{\text{shunt}}(p) = \begin{bmatrix} 1 & 0 \\ y(p) & 1 \end{bmatrix}$$

using the using the impedance  $z(p)$  and admittance  $y(p)$ . Connecting the series and shunts in a “chain” produces a 2-port called a ladder. The ladder’s chain matrix is the product of the individual chain matrices of the series and shunt 2-ports. For example, the low-pass ladders are a classic family of lossless matching

2-ports. Figure 11 shows a low-pass ladder with Port 2 terminated in a load  $z_L$ . The low-pass ladder has chain matrix

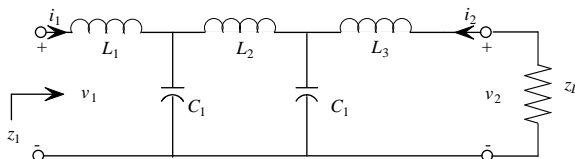


**Figure 11.** A low-pass ladder terminated in a load.

$$T(p) = \begin{bmatrix} 1 & pL_1 \\ 0 & 1 \end{bmatrix} \begin{bmatrix} 1 & 0 \\ pC_1 & 1 \end{bmatrix} \begin{bmatrix} 1 & pL_2 \\ 0 & 1 \end{bmatrix} \begin{bmatrix} 1 & 0 \\ pC_2 & 1 \end{bmatrix} \begin{bmatrix} 1 & pL_3 \\ 0 & 1 \end{bmatrix}.$$

The impedance looking into Port 1 is computed

$$z_1 = \frac{v_1}{i_1} = \frac{t_{11}z_L + t_{12}}{t_{21}z_L + t_{22}} =: \mathfrak{G}(T, z_L).$$

Thus, the chain matrices provide a natural parameterization for the *orbit of the load  $z_L$  under the action of the low-pass ladders*. Section 1 showed that these orbits are fundamental for the matching problem. Even at this elementary level, the mathematician can raise some pretty substantial questions regarding how these ladders sit in  $U^+(2)$  or how the orbit of the load sits in the unit ball of  $H^\infty$ .

Unfortunately, the impedance, the admittance, and the chain formalisms do not provide ideal representations for all circuits of interest. For example, there are  $N$ -ports that do not have an impedance matrix (i.e., the transformer does not have an impedance matrix). There are difficulties inherent in attempting the matching problem in a formalism where the some of the basic objects under discussion fail to exist.

In fact, much of the debate in electrical engineering in the 1960's focused on finding the right formalism that guaranteed that every  $N$ -port had a representation as the graph of a linear operator. For example, the existence of the impedance matrix  $Z(p)$  is equivalent to

$$\mathcal{N} = \left\{ \begin{bmatrix} Z\mathbf{i} \\ \mathbf{i} \end{bmatrix} : \mathbf{i} \in L^2(j\mathbb{R}, \mathbb{C}^N) \right\}.$$

but this formalism is not so useful when we need to describe circuits with transformers in them. The claim is that any linear, passive, time-invariant, solvable  $N$ -port always admits a *scattering matrix*  $S \in \bar{B}H^\infty(\mathbb{C}_+, \mathbb{C}^{N \times N})$ ; see [3; 4; 31]. Consequently, we work the matching problem in the scattering formalism, which we now describe.

**4.2. The scattering matrices.** Specializing to the 2-port in Figure 12, define

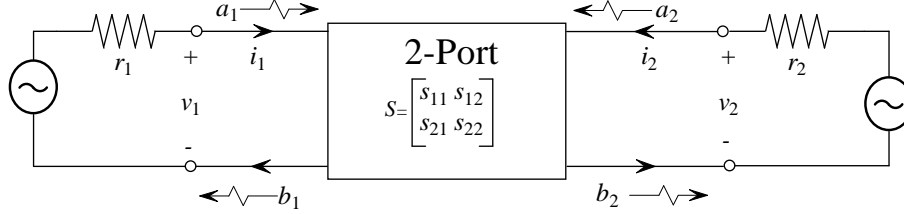


**Figure 12.** The 2-port scattering formalism.

the *incident signal* (see [3, Eq. 4.25a] and [4, page 234]):

$$\mathbf{a} = \frac{1}{2}\{R_0^{-1/2}\mathbf{v} + R_0^{1/2}\mathbf{i}\} \quad (4-2)$$

and the *reflected signal* (see [3, Eq. 4.25b] and [4, page 234]):

$$\mathbf{b} = \frac{1}{2}\{R_0^{-1/2}\mathbf{v} - R_0^{1/2}\mathbf{i}\}, \quad (4-3)$$

with respect to the normalizing<sup>1</sup> matrix

$$R_0 = \begin{bmatrix} r_1 & 0 \\ 0 & r_2 \end{bmatrix}.$$

The scattering matrix maps the incident wave to the reflected wave:

$$\mathbf{b} = \begin{bmatrix} b_1 \\ b_2 \end{bmatrix} = \begin{bmatrix} s_{11} & s_{12} \\ s_{21} & s_{22} \end{bmatrix} \begin{bmatrix} a_1 \\ a_2 \end{bmatrix} = S\mathbf{a}.$$

The scattering description can be readily related to other representations when the latter exist. For instance, the scattering matrix determines the impedance matrix as

$$\tilde{Z} := R_0^{-1/2}ZR_0^{-1/2} = (I + S)(I - S)^{-1}.$$

To see this, invert Equations 4-2 and 4-3 and substitute into  $\mathbf{v} = Z\mathbf{i}$ . Conversely, if the  $N$ -port admits an impedance matrix, normalize and Cayley transform to get

$$S = (\tilde{Z} - I)(\tilde{Z} + I)^{-1}.$$

Usually,  $R_0 = r_0I$  with  $r_0 = 50$  ohms so the normalizing matrix disappears. The math guys always take  $r_0 = 1$ . The EE's have endless arguments about normalizations. Unless stated otherwise, we'll always normalize with respect to  $r_0$ .

<sup>1</sup>Two accessible books on the scattering parameters are [3] and [4]. The first of these omits the factor  $\frac{1}{2}$  but carries this rescaling onto the power definitions. Most other books use the *power-wave normalization* [16]:  $\mathbf{a} = R_0^{-1/2}\{\mathbf{v} + Z_0\mathbf{i}\}/2$ , where the normalizing matrix  $Z_0 = R_0 + jX_0$  is diagonal with diagonal resistance  $R_0 > 0$  and reactance  $X_0$ .

**4.3. The chain scattering matrix.** Closely related to the scattering matrix is the *chain scattering matrix*  $\Theta$  [25, page 148]:

$$\begin{bmatrix} b_1 \\ a_1 \end{bmatrix} = \Theta \begin{bmatrix} a_2 \\ b_2 \end{bmatrix} = \begin{bmatrix} \theta_{11} & \theta_{12} \\ \theta_{21} & \theta_{22} \end{bmatrix} \begin{bmatrix} a_2 \\ b_2 \end{bmatrix}.$$

When multiple 2-ports are connected in a chain the chain scattering matrix of the chain is the product of the individual chain scattering matrices. The mappings between the scattering and chain scattering matrices are [25]:

$$S \mapsto s_{21}^{-1} \begin{bmatrix} -\det[S] & s_{11} \\ -s_{22} & 1 \end{bmatrix} = \Theta \mapsto \theta_{22}^{-1} \begin{bmatrix} \theta_{12} & \det[\Theta] \\ 1 & -\theta_{21} \end{bmatrix} = S. \quad (4-4)$$

Although every 2-port has a scattering matrix, it admits chain scattering matrix only if  $s_{21}$  is invertible.

**4.4. Passive terminations.** In Figure 6, Port 2 is terminated with the load reflectance  $s_L$  so that

$$a_2 = s_L b_2. \quad (4-5)$$

Then the reflectance looking into Port 1 is obtained by the chain-scattering matrix:

$$s_1 := \frac{b_1}{a_1} = \frac{\theta_{11}a_2 + \theta_{12}b_2}{\theta_{21}a_2 + \theta_{22}b_2} = \frac{\theta_{11}s_L + \theta_{12}}{\theta_{21}s_L + \theta_{22}} =: \mathcal{G}_1(\Theta, s_L).$$

Equation 4-4 also allows us to express  $s_1$  in terms of the linear-fractional form of the scattering matrix introduced in Equation 2-2:  $s_1 = \mathcal{F}_1(S, s_L)$ . Similarly, if Port 1 of the 2-port is terminated with the load reflectance  $s_G$ , then the reflectance looking into Port 2 is

$$s_2 = \mathcal{G}_2(\Theta, s_G) := \frac{\theta_{22}s_G + \theta_{21}}{\theta_{12}s_G + \theta_{11}} = \mathcal{F}_2(S, s_G),$$

with  $\mathcal{F}_2(S, s_G)$  as introduced in Equation 2-3.

**4.5. Active terminations.** Equation 4-5 admits a generalization to include the generators. Figure 13 shows the labeling convention of the scattering variables. The generalization includes the scattering of the generator in terms of the

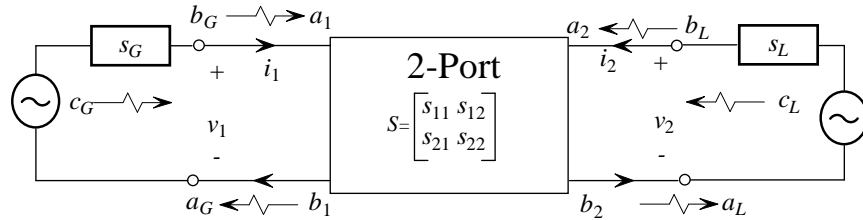


**Figure 13.** Scattering conventions.

voltage source [16, Eq. 3.2]:

$$b_G = s_G a_G + c_G; \quad c_G := \frac{r_0^{-1/2}}{z_G + r_0} v_G. \quad (4-6)$$

To get this result, use Equations 4-2 and 4-3 to write  $v_1 = r_0^{1/2}(a_1 + b_1)$  and  $i_1 = r_0^{-1/2}(a_1 - b_1)$ . Substitute this into the voltage drops  $v_G = z_G i_1 + v_1$  of Figure 13 to get

$$c_G = \frac{r_0^{-1/2} v_G}{z_G + r_0} = a_1 - \frac{z_G - r_0}{z_G + r_0} b_1 = b_G - s_G a_G.$$

We can now analyze the setup in Figure 13. Equations 4-5 and 4-6 give

$$\mathbf{a} = \begin{bmatrix} a_1 \\ a_2 \end{bmatrix} = \begin{bmatrix} s_G & 0 \\ 0 & s_L \end{bmatrix} \begin{bmatrix} b_1 \\ b_2 \end{bmatrix} + \begin{bmatrix} c_G \\ c_L \end{bmatrix} =: S_X \mathbf{b} + \mathbf{c}_X.$$

Substitution into  $\mathbf{b} = S\mathbf{a}$  solves the 2-port scattering as

$$\mathbf{a} = (I_2 - S_X S)^{-1} \mathbf{c}_X.$$

**4.6. Power flows in the 2-port.** With respect to an  $N$ -port, the complex power<sup>2</sup> is [4, page 241]:

$$W(p) := \mathbf{v}(p)^H \mathbf{i}(p).$$

Because  $\mathbf{v}(p)$  has units volts second and  $\mathbf{i}(p)$  has units ampères second,  $W(p)$  units of watts/Hz<sup>2</sup>. The average power delivered to the  $N$ -port is [21, page 19]

$$P_{\text{avg}} := \frac{1}{2} \text{Re}[W] = \frac{1}{2} \{\mathbf{a}^H \mathbf{a} - \mathbf{b}^H \mathbf{b}\} = \frac{1}{2} \mathbf{a}^H \{I - S^H S\} \mathbf{a}. \quad (4-7)$$

We're dragging the 1/2 along so our power definitions coincide with [21]. If the  $N$ -port consumes power ( $P_{\text{avg}} \geq 0$ ) for all its voltage and current pairs, then the  $N$ -port is said to be passive. If the  $N$ -port consumes no power ( $P_{\text{avg}} = 0$ ) for all its voltage and current pairs, then the  $N$ -port is said to be lossless. In terms of the scattering matrices [28]:

- Passive:  $S^H(j\omega)S(j\omega) \leq I_N$
- Lossless:  $S^H(j\omega)S(j\omega) = I_N$

for all  $\omega \in \mathbb{R}$ . Specializing these concepts to the 2-port of Figure 14, leads to the following power flows:

- The average power delivered to Port 1 is

$$P_1 := \frac{1}{2} (|a_1|^2 - |b_1|^2) = \frac{|a_1|^2}{2} (1 - |s_1|^2).$$

- The average power delivered to Port 2 is

$$P_2 := \frac{1}{2} (|a_2|^2 - |b_2|^2) = -P_L.$$

<sup>2</sup>Baher uses [3, Eq. 2.17]:  $W(p) = \mathbf{i}(p)^H \mathbf{v}(p)$ .

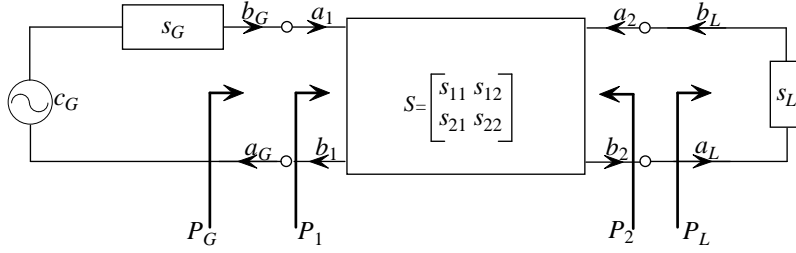


**Figure 14.** Matching circuit and reflectances.

- The average power delivered to the load is [21, Eq. 2.6.6]

$$P_L := \frac{1}{2}(|a_L|^2 - |b_L|^2) = \frac{|b_2|^2}{2}(1 - |s_L|^2).$$

- The average power delivered by the generator:

$$P_G = \frac{1}{2}(|b_G|^2 - |a_G|^2).$$

To compute  $P_G$ , observe that Figure 14 gives  $a_G = b_1$  and  $b_G = a_1$ . Substitute these and  $b_1 = s_1 a_1$  into Equation 4-6 to get  $c_G = (1 - s_G s_1) a_1$ . Then

$$P_G = \frac{1}{2}(|a_1|^2 - |b_1|^2) = \frac{|a_1|^2}{2}(1 - |s_1|^2) = \frac{|c_G|^2}{2} \frac{1 - |s_1|^2}{|1 - s_G s_1|^2}. \quad (4-8)$$

LEMMA 4.1. *Assume the setup of Figure 14. There always holds  $P_2 = -P_L$  and  $P_G = P_1$ . If the 2-port is lossless,  $P_1 + P_2 = 0$ .*

**4.7. The power gains in the 2-port.** The matching network maps the generator's power into a form that we hope will be more useful at the load than if the generator drove the load directly. The modification of power is generically described as "gain." The matching problem puts us in the business of gain computations, and we need the maximum power and mismatch definitions. The maximum power available from a generator is defined as the average power delivered by the generator to a conjugately matched load. Use Equation 4-8 to get [21, Eq. 2.6.7]:

$$P_{G,\max} := P_G|_{s_1=\bar{s}_G} = \frac{|c_G|^2}{2}(1 - |s_G|^2)^{-1}.$$

The *source mismatch factor* is [21, Eq. 2.7.17]:

$$\frac{P_G}{P_{G,\max}} = \frac{(1 - |s_G|^2)(1 - |s_1|^2)}{|1 - s_G s_1|^2}.$$

The maximum power available from the matching network is defined as the average power delivered from the network to a conjugately matched load [21, Eq. 2.6.19]:

$$P_{L,\max} := P_L|_{s_L=\bar{s}_2} = \frac{|b_2|_{s_L=\bar{s}_2}^2}{2}(1 - |s_2|^2).$$

Less straightforward to derive is the *load mismatch factor* [21, Eq. 2.7.25]:

$$\frac{P_L}{P_{L,\max}} = \frac{(1 - |s_L|^2)(1 - |s_2|^2)}{|1 - s_L s_2|^2}.$$

These powers lead to several types of power gains [21, page 213]:

- Transducer power gain

$$G_T := \frac{P_L}{P_{G,\max}} = \frac{\text{power delivered to the load}}{\text{maximum power available from the generator}}.$$

- Power gain or operating power gain

$$G_P := \frac{P_L}{P_1} = \frac{\text{power delivered to the load}}{\text{power delivered to the network}}.$$

- Available power gain

$$G_A := \frac{P_{L,\max}}{P_{G,\max}} = \frac{\text{maximum power available from the network}}{\text{maximum power available from the generator}}.$$

LEMMA 4.2. *Assume the setup of Figure 14. If the 2-port is lossless,*

$$G_T = \frac{(1 - |s_G|^2)(1 - |s_1|^2)}{|1 - s_G s_1|^2}.$$

PROOF.

$$G_T = \frac{P_L}{P_{G,\max}} \stackrel{\text{Lemma 4.1}}{=} \frac{-P_2}{P_{G,\max}} \stackrel{\text{lossless}}{=} \frac{P_1}{P_{G,\max}} \stackrel{\text{Lemma 4.1}}{=} \frac{P_G}{P_{G,\max}}.$$

□

What's nice about the proof is that it makes clear that the equality holds because the power flowing into the lossless 2-port is the power flowing out of the 2-port. The key to analyzing the transducer power gain is the power mismatch.

**4.8. Power mismatch.** Previously we established that the power mismatch is the key to the matching problem. In fact, this is a concept that brings together ideas from pure mathematics and applied electrical engineering, as seen in the engineer's Smith Chart — a disk-shaped analysis tool marked with coordinate curves which look compellingly familiar to the mathematician. A standard engineering reference observes the connection [51]:

The transformation through a lossless junction [2-port] . . . leaves invariant the *hyperbolic distance* . . . The hyperbolic distance to the origin of the [Smith] chart is the *mismatch*, that is, the standing-wave ratio expressed in decibels: It may be evaluated by means of the proper graduation on the radial arm of the Smith chart. For two arbitrary points  $W_1$ ,  $W_2$ , the hyperbolic distance between them may be interpreted as the mismatch that results from the load  $W_2$  seen through a lossless network that matches  $W_1$  to the input waveguide.

Hyperbolic metrics have been under mathematical development for the last 200 years, while Phil Smith introduced his chart in the late 1930's with a somewhat different motivation. It is fascinating to see how hyperbolic analysis transcribes to electrical engineering. Mathematically, we start with the *pseudohyperbolic metric*<sup>3</sup> on  $\mathbf{D}$  defined as follows (see [58, page 58]):

$$\rho(s_1, s_2) := \left| \frac{s_1 - s_2}{1 - \bar{s}_1 s_2} \right| \quad (s_1, s_2 \in \mathbf{D}).$$

The Möbius group of symmetries of  $\mathbf{D}$  consists of all maps  $\mathbf{g} : \mathbf{D} \rightarrow \mathbf{D}$  [20, Theorem 1.3]:

$$\mathbf{g}(s) = e^{j\theta} \frac{s - a}{1 - \bar{a}s},$$

where  $a \in \mathbf{D}$  and  $\theta \in \mathbb{R}$ . That  $\rho$  is invariant under the Möbius maps  $\mathbf{g}$  is fundamental (see [20] and [58, page 58]):

$$\rho(\mathbf{g}(s_1), \mathbf{g}(s_2)) = \rho(s_1, s_2). \quad (4-9)$$

The *hyperbolic metric*<sup>4</sup> on  $\mathbf{D}$  is [58, page 59]:

$$\beta(s_1, s_2) = \frac{1}{2} \log \left( \frac{1 + \rho(s_1, s_2)}{1 - \rho(s_1, s_2)} \right).$$

Because  $\rho$  is Möbius-invariant, it follows that  $\beta$  is also Möbius-invariant:

$$\beta(\mathbf{g}(s_1), \mathbf{g}(s_2)) = \beta(s_1, s_2).$$

One can visualize the matching problem in terms of the action of this group of symmetries. At fixed frequency, a given load reflectance  $s_L$  corresponds to a point in  $\mathbf{D}$ . Attaching a matching network to the load modifies this reflectance by applying to it the Möbius transformation associated with the chain scattering matrix of the matching network. By varying the choice of the matching network, we vary the Möbius map applied to  $s_L$  and sweep the modified reflectance around the disk to a desirable position.

The series inductor of Figure 10 provides an excellent example of this action of a circuit as Möbius map acting on the reflectances parameterized as points of the unit disk. The series inductor has the chain scattering matrix [25, Table 6.2]:

$$\Theta(p) = \begin{bmatrix} 1 - Lp/2 & Lp/2 \\ -Lp/2 & 1 + Lp/2 \end{bmatrix}.$$

that acts on  $s \in \mathbf{D}$  as

$$\mathcal{G}(\Theta; s) = \frac{\Theta_{11}s + \Theta_{12}}{\Theta_{21}s + \Theta_{22}} = -\frac{\bar{a}}{a} \frac{s - a}{1 - \bar{a}s} \Big|_{a=(1+j2/(\omega L))^{-1}}.$$

<sup>3</sup>Also known as the Poincaré hyperbolic distance function; see [50].

<sup>4</sup>Also known as the Bergman metric or the Poincaré metric.

Figure 15 shows the Möbius action of this lossless 2-port on the disk. Frequency is fixed at  $p = j$ . The upper left panel shows the unit disk partitioned into radial segments. Each of the other panels show the action of an inductor on the points of this disk. Increasing the inductance warps the radial pattern to the boundary. The radial segments are geodesics of  $\rho$  and  $\beta$ . Because the Möbius maps preserve both metrics, the resulting circles are also geodesics. More generally, the geodesics of  $\rho$  and  $\beta$  are either the radial lines or the circles that meet the boundary of the unit disk at right angles.

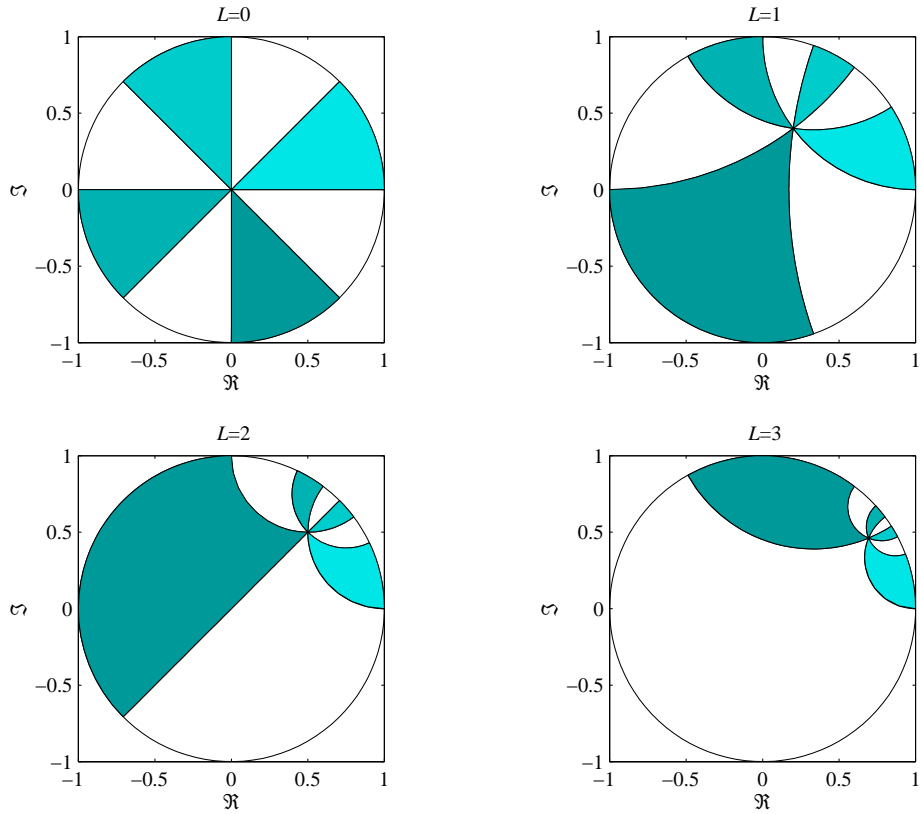


**Figure 15.** Möbius action of the series inductor on the unit disk for increasing inductance values (frequency fixed at  $p = j$ ).

Several electrical engineering figures of merit for the matching problem are naturally understood in terms of the geometry of the hyperbolic disk. We are concerned primarily with three: (1) the power mismatch, (2) the VSWR, (3) the transducer power gain. The power mismatch between two passive reflectances  $s_1, s_2$  is [29]:

$$\Delta P(s_1, s_2) := \left| \frac{\bar{s}_1 - s_2}{1 - s_1 s_2} \right| = \rho(\bar{s}_1, s_2), \quad (4-10)$$

or the pseudohyperbolic distance between  $\bar{s}_1$  and  $s_2$  measured along their geodesic. Thus, the geodesics of  $\rho$  attach a geometric meaning to the power mismatch and illustrate the quote at the beginning of this section.

The voltage standing wave ratio (VSWR) is a sensitive measure of impedance mismatch. Intuitively, when power is pushed into a mismatched load, part of the power is reflected back measured by the reflectance  $s \in \mathbf{D}$ . Superposition of the incident and reflected wave sets up a voltage standing wave pattern. The VSWR is the ratio of the maximum to minimum voltage in this pattern: [6, Equation 3.51]:

$$\text{VSWR}(s) = 20 \log_{10} \left( \frac{1 + |s|}{1 - |s|} \right) \quad [\text{dB}].$$

Referring to Figure 15, the VSWR is a scaled hyperbolic distance from the origin to  $s$  measured along its radial line. Thus, the geodesics of  $\beta$  attach a geometric meaning to the VSWR.

The transducer power gain  $G_T$  links to the power mismatch  $\Delta P$  by the classical identity of the hyperbolic metric [58, page 58]:

$$1 - \rho(s_1, s_2)^2 = \frac{(1 - |s_1|^2)(1 - |s_2|^2)}{|1 - \bar{s}_1 s_2|^2} \quad (s_1, s_2 \in \mathbf{D}), \quad (4-11)$$

and Lemma 4.2 provided the matching 2-port is lossless.

LEMMA 4.3. *If the 2-port is lossless in Figure 14,  $G_T = 1 - \Delta P(s_G, s_1)^2$ .*

That is, *maximizing  $G_T$  is equivalent to minimizing the power mismatch*. As the next result shows, we can use either Port 1 or Port 2 (Proof in Appendix B).

LEMMA 4.4. *Assume the 2-port is lossless in Figure 6:  $S \in U^+(2)$ . Assume  $s_G$  and  $s_L$  are strictly passive:  $s_G, s_L \in BH^\infty(\mathbb{C}_+)$ . Then  $s_1 = \mathcal{F}_1(S, s_L)$  and  $s_2 = \mathcal{F}_2(S, s_G)$  (defined in Equations 2-2 and 2-3 respectively) are well-defined and strictly passive with the LFT (Linear Fractional Transform) law*

$$\Delta P(s_G, \mathcal{F}_1(S, s_L)) = \Delta P(\mathcal{F}_2(S, s_G), s_L)$$

and the TPG (Transducer Power Gain) law

$$G_T(s_G, S, s_L) = 1 - \Delta P(s_G, \mathcal{F}_1(S, s_L))^2 = 1 - \Delta P(\mathcal{F}_2(S, s_G), s_L)^2$$

holding on  $j\mathbb{R}$ .

The LFT law is not true if  $S$  is strictly passive. For  $S^H S < I_2$ , define the gains at Port 1 and 2 as follows:

$$G_1(s_G, S, s_L) := 1 - \Delta P(s_G, \mathcal{F}_1(S, s_L))^2$$

$$G_2(s_G, S, s_L) := 1 - \Delta P(\mathcal{F}_2(S, s_G), s_L)^2.$$

Lemma 4.4 gives that  $G_T = G_1 = G_2$ , provided  $S$  is lossless. If  $S$  is only passive, we can only say  $G_T \leq G_1, G_2$ . To see this, Equation 4–11 identifies  $G_1$  and  $G_2$  as mismatch factors:

$$G_1(s_G, S, s_L) = 1 - \Delta P(s_G, s_1)^2 = \frac{P_G}{P_{G,\max}},$$

$$G_2(s_G, S, s_L) := 1 - \Delta P(s_2, s_L)^2 = \frac{P_L}{P_{L,\max}}.$$

If we believe that a passive 2-port forces the available gain  $G_A \leq 1$  and power gain  $G_P \leq 1$  of Section 4.7, the inequalities  $G_T \leq G_1, G_2$  are explained as

$$G_T = \frac{P_L}{P_{G,\max}} = \frac{P_{L,\max}}{P_{G,\max}} \frac{P_L}{P_{L,\max}} = G_A G_2$$

$$G_T = \frac{P_L}{P_{G,\max}} = \frac{P_1}{P_{G,\max}} \frac{P_L}{P_1} = G_P G_1.$$

**4.9. Sublevel sets of the power mismatch.** We have just seen that impedance matching reduces to minimization of the power mismatch. We can obtain some geometrical intuition for the behavior of this by examining Figure 16, which shows the isocontours of the function  $s_2 \mapsto \Delta P(s_2, s_L)$  for a fixed reflectance  $s_L$  in the unit disk (at a fixed frequency). The key observation is that for each fixed frequency, the sublevel sets  $\{s_2 \in \mathbf{D} : \Delta P(s_2, s_L) \leq \rho\}$  comprise a family of concentric disks with hyperbolic center  $\bar{s}_L$ . Of course, we must actually consider power mismatch over a range of frequencies. To this end, the next lemma characterizes the corresponding sublevel sets in  $L^\infty(j\mathbb{R})$ .

LEMMA 4.5 ( $\Delta P$  DISKS). *Let  $s_L \in BL^\infty(j\mathbb{R})$ . Let  $0 \leq \rho \leq 1$ . Define the center function*

$$k := \bar{s}_L \frac{1 - \rho^2}{1 - \rho^2 |s_L|^2} \in BL^\infty(j\mathbb{R}), \quad (4-12)$$

*the radius function*

$$r := \rho \frac{1 - |s_L|^2}{1 - \rho^2 |s_L|^2} \in \bar{BL}^\infty(j\mathbb{R}), \quad (4-13)$$

*and the disk*

$$\bar{D}(k, r) := \{\phi \in L^\infty(j\mathbb{R}) : |\phi(j\omega) - k(j\omega)| \leq r(j\omega)\}.$$

*Then,*

D-1:  $\bar{D}(k, r)$  is a closed, convex subset of  $L^\infty(j\mathbb{R})$ .

D-2:  $\bar{D}(k, r) = \{\phi \in \bar{BL}^\infty(j\mathbb{R}) : \rho \geq \|\Delta P(\phi, s_L)\|_\infty\}$ .

D-3:  $\bar{D}(k, r)$  is a weak-\* compact, convex subset of  $L^\infty(j\mathbb{R})$ .

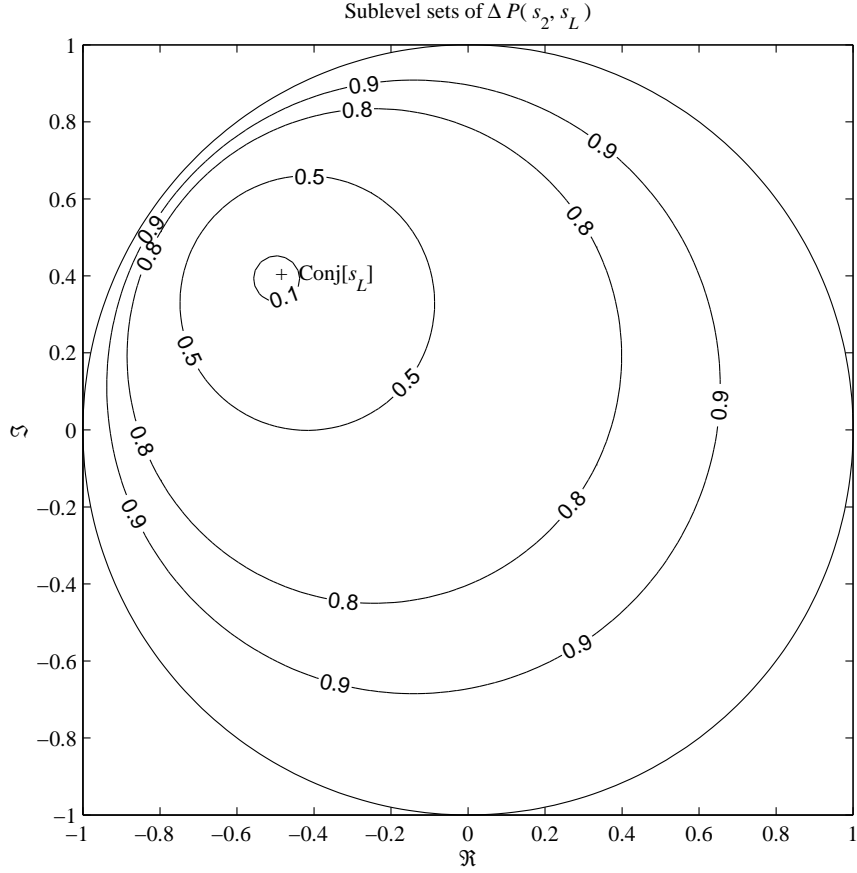


**Figure 16.** Sublevel sets of  $\Delta P(s_2, s_L)$  in the unit disk.

PROOF. Under the assumption that  $\|s_L\|_\infty < 1$ , it is straightforward to verify that the center and radius functions are in the open and closed unit balls of  $L^\infty(j\mathbb{R})$ , respectively.

**D-1:** Convexity and closure follow from pointwise convexity and closure.

**D-2:** Basic algebra computes  $\bar{D}(k, r) = \{\phi \in L^\infty(j\mathbb{R}) : \rho \geq \|\Delta P(\phi, s_L)\|_\infty\}$ . The “free” result is that  $\|\bar{D}(k, r)\|_\infty \leq 1$ . To see this, let  $s := \|s_L\|_\infty$ . The norm of any element in  $\bar{D}(k, r)$  is bounded by

$$\|k\|_\infty + \|r\|_\infty \leq s \frac{1 - \rho^2}{1 - \rho^2 s^2} + \rho \frac{1 - s^2}{1 - \rho^2 s^2} =: u(s, \rho).$$

For  $s \in [0, 1)$  fixed, we obtain

$$\frac{\partial u}{\partial \rho} = -\frac{-1 + s^2}{(\rho s + 1)^2}.$$

Thus,  $u(s, \circ)$  attains its maximum on the boundary of  $[0, 1]$ :  $u(s, 1) = 1$ . Thus,  $\|\bar{D}(k, r)\|_\infty \leq 1$ .

**D-3:** D-1 and Lemma 3.2. □

**4.10. Continuity of the power mismatch.** Consider the mapping  $\Delta\rho : \bar{B}L^\infty(j\mathbb{R}) \rightarrow \mathbb{R}_+$

$$\Delta\rho(s_2) := \|\Delta P(s_2, s_L)\|_\infty,$$

for fixed  $s_L \in BL^\infty(j\mathbb{R})$ . The main problem of this paper concerns the minimization of this functional over feasible classes (ultimately, the orbits of the reflectance under classes of matching circuits). This problem is determined by the structure of the sublevel sets of  $\Delta\rho$ . What we have just seen is that the sublevel sets are disks in function space, a very nice structure indeed. As the “level” of  $\Delta\rho$  is decreased, these sets neck down; the question of existence of a minimizer in a feasible class comes down to the intersection of the feasible class with these sublevel sets.

**DEFINITION 4.1.** [48, pages 38–39], [57, page 150] Let  $\gamma$  be a real or extended-real function on a topological space  $X$ .

- $\gamma$  is lower semicontinuous provided  $\{x \in X : \gamma(x) \leq \alpha\}$  is closed for every real  $\alpha$ .
- $\gamma$  is lower semicompact provided  $\{x \in X : \gamma(x) \leq \alpha\}$  is compact for every real  $\alpha$ .

These properties produce minimizers by the Weierstrass Theorem.

**THEOREM 4.1 (WEIERSTRASS).** [57, page 152] *Let  $K$  be a nonempty subset of a topological space  $X$ . Let  $\gamma$  be a real or extended-real function defined on  $K$ . If either condition holds:*

- $\gamma$  is lower semicontinuous on the compact set  $K$ , or
- $\gamma$  is lower semicompact,

*then  $\inf\{\gamma(x) : x \in K\}$  admits minimizers.*

Lemma 4.5 demonstrates that  $\Delta\rho$  is both weak-\* lower semicontinuous and weak-\* lower compact. The minimum of  $\Delta\rho$  in  $\bar{B}L^\infty(j\mathbb{R})$  is  $0 = \Delta\rho(\bar{s}_L)$  that corresponds to a perfect match over all frequencies. However, the matching functions at our disposal are not arbitrary, and this trivial solution is typically not obtainable with real matching circuits. The constraints on allowable matching functions lead us to consider minimizing  $\Delta\rho$  restricted to  $\bar{B}H^\infty(\mathbb{C}_+)$ ,  $\bar{B}A_1(\mathbb{C}_+)$ , and associated orbits. Finally, straight-forward sequence arguments show that  $\Delta\rho$  is also continuous as a function on  $\bar{B}L^\infty(j\mathbb{R})$  in the norm topology.

**LEMMA 4.6.** *If  $s_L \in BL^\infty(j\mathbb{R})$ , then  $\Delta\rho : \bar{B}L^\infty(j\mathbb{R}) \rightarrow \mathbb{R}_+$  is continuous.*

**PROOF.** Define  $\Delta P_1 : \bar{B}L^\infty(j\mathbb{R}) \rightarrow L^\infty(j\mathbb{R})$  as  $\Delta P_1(s) := (\bar{s} - s_L)(1 - ss_L)^{-1}$ . If we show that  $\Delta P_1$  is continuous then composition with  $\|\circ\|_\infty$  shows continuity

of  $\Delta\rho$ . The first task is to show  $\Delta P_1$  is well-defined. For each  $s \in \bar{B}L^\infty(j\mathbb{R})$ ,  $\Delta P_1(s)$  is measurable and

$$\left| \frac{\bar{s} - s_L}{1 - s s_L} \right| \leq \frac{2}{1 - \|s\|_\infty \|s_L\|_\infty} \leq \frac{2}{1 - \|s_L\|_\infty}.$$

Thus,  $\Delta P_1(s) \in L^\infty(j\mathbb{R})$  so is well-defined. For continuity, let  $\{s_n\} \subset \bar{B}L^\infty(j\mathbb{R})$  and  $s_n \rightarrow s$ . Then

$$\begin{aligned} \Delta P_1(s_n) - \Delta P_1(s) &= \frac{\bar{s}_n - s_L}{1 - s_n s_L} - \frac{\bar{s} - s_L}{1 - s s_L} \\ &= \frac{1}{(1 - s_n s_L)(1 - s s_L)} \{(\bar{s}_n - s_L)(1 - s s_L) - (\bar{s} - s_L)(1 - s_n s_L)\} \\ &= \frac{1}{(1 - s_n s_L)(1 - s s_L)} \{\overline{s_n - s} + s_L(\bar{s} s_n - \bar{s}_n s) + (s - s_n)s_L^2\}. \end{aligned}$$

In terms of the norm,

$$\begin{aligned} \|\Delta P_1(s_n) - \Delta P_1(s)\| &\leq (1 - \|s_L\|_\infty)^{-2} \{\|\overline{s_n - s}\|_\infty + \|s_L\|_\infty \|\bar{s} s_n - \bar{s}_n s\|_\infty + \|s - s_n\|_\infty \|s_L\|_\infty^2\}, \end{aligned}$$

so that the difference converges to zero. With  $\Delta P_1$  a continuous mapping, the continuity of the norm  $\|\circ\|_\infty : L^\infty(j\mathbb{R}) \rightarrow \mathbb{R}_+$  makes the mapping  $\Delta\rho(s) := \|\Delta P_1(s)\|_\infty$  also continuous.  $\square$

## 5. $H^\infty$ Matching Techniques

Recalling the matching problem synopsis of Section 2, our goal is to maximize the transducer power gain  $G_T$  over a specified class  $\mathcal{U}$  of scattering matrices. By Lemma 4.3, we can equivalently minimize the power mismatch:

$$\begin{aligned} \sup\{\|G_T(s_G, S, s_L)\|_{-\infty} : S \in \mathcal{U}\} &= 1 - \inf\{\|\Delta P(\mathcal{F}_2(S, s_G), s_L)\|_\infty^2 : S \in \mathcal{U}\} \\ &= 1 - \inf\{\|\Delta P(s_2, s_L)\|_\infty^2 : s_2 \in \mathcal{F}_2(\mathcal{U}, s_G)\} \\ &\leq 1 - \inf\{\|\Delta P(s_2, s_L)\|_\infty^2 : s_2 \in \bar{B}H^\infty(\mathbb{C}_+)\}. \end{aligned}$$

The next step in our program is to develop tools for computing the upper bound at the end of this chain of expressions, based on what we know of  $s_L$ . Ultimately, we will try to make this a tight bound given the right properties of the admissible matching circuits parameterized by  $\mathcal{U}$ . The key computation is a hyperbolic version of Nehari's Theorem that computes the minimum power mismatch from the Hankel matrix determined by  $s_L$ .

We start towards this in Section 5.1 by reviewing the concept of Hankel operators and their relation to best approximation from  $H^\infty$  as expressed by the linear Nehari theory. Section 5.2 extends this to a nonlinear framework that includes the desired hyperbolic Nehari bound on the power mismatch as a special case.

Having computed a bound on our ability to match a given load, we consider how closely one can approach this in a practical implementation with real circuits. The key matching circuits we consider in practice are the lumped, lossless 2-ports with scattering matrices in  $U^+(2, \infty)$ . Later on, Section 7 demonstrates that the orbit of  $s_G = 0$  under  $U^+(2, \infty)$  is dense in the real disk algebra,  $\text{Re } \bar{B}\mathcal{A}_1(\mathbb{C}_+)$  (Darlington's Theorem), so that smallest mismatch approachable with lumped circuits is

$$\begin{aligned} & \inf\{\|\Delta P(s_2, s_L)\|_\infty : s_2 \in \mathcal{F}_2(U^+(2, \infty), 0)\} \\ &= \inf\{\|\Delta P(s_2, s_L)\|_\infty : s_2 \in \text{Re } \bar{B}\mathcal{A}_1(\mathbb{C}_+)\}. \end{aligned}$$

If we can relate the latter infimum to the minimization over the larger space  $H^\infty(\mathbb{C}_+)$ , then minimizing the power mismatch over the lumped circuits can be related to the computable hyperbolic Nehari bound. This seems plausible from experience with the classical linear Nehari Theory, where  $\phi$  real and continuous implies that the distance from the real subset of disk algebra is the same as the distance to  $H^\infty$ :

$$\|\phi - H^\infty(\mathbb{C}_+)\|_\infty = \|\phi - \text{Re } \mathcal{A}_1(\mathbb{C}_+)\|_\infty.$$

Section 5.3 obtains similar results for the nonlinear hyperbolic Nehari bound using metric properties of the power mismatch  $\Delta P$ .

Thus, the results of this section will provide the desired result: the Nehari bound for the matching problem is both computable and tight in the sense that a sequence of lumped, lossless 2-ports can be found that approach the Nehari bound.

**5.1. Nehari's theorem.** The Toeplitz and Hankel operators are most conveniently defined on  $L^2(\mathbf{T})$  using the Fourier basis. Let  $\phi \in L^2(\mathbf{T})$  have the Fourier expansion

$$\phi(z) = \sum_{n=-\infty}^{\infty} \hat{\phi}(n) z^n \quad (z = e^{j\theta}).$$

Let  $P$  denote the orthogonal projection of  $L^2(\mathbf{T})$  onto  $H^2(\mathbf{D})$ :

$$P\phi(z) = \sum_{n=0}^{\infty} \hat{\phi}(n) z^n.$$

The *Toeplitz operator* with symbol  $\phi \in L^\infty(\mathbf{T})$  is the mapping  $\mathcal{T}_\phi : H^2(\mathbf{D}) \rightarrow H^2(\mathbf{D})$

$$\mathcal{T}_\phi h := P(\phi h).$$

The *Hankel operator* with symbol  $\phi \in L^\infty(\mathbf{T})$  is the mapping  $\mathcal{H}_\phi : H^2(\mathbf{D}) \rightarrow H^2(\mathbf{D})$

$$\mathcal{H}_\phi h := U(I - P)(\phi h),$$

where  $U : H^2(\mathbf{D})^\perp \rightarrow H^2(\mathbf{D})$  is the unitary “flipping” operator:

$$Uh(z) := z^{-1}h(z^{-1}).$$

These operators admit matrix representations with respect to the Fourier basis [56, page 173]:

$$\mathcal{J}_\phi = \begin{bmatrix} \widehat{\phi}(0) & \widehat{\phi}(1) & \widehat{\phi}(2) & \ddots \\ \widehat{\phi}(-1) & \widehat{\phi}(0) & \widehat{\phi}(1) & \ddots \\ \widehat{\phi}(-2) & \widehat{\phi}(-1) & \widehat{\phi}(0) & \ddots \\ \vdots & \vdots & \vdots & \ddots \end{bmatrix}$$

and [56, page 191]

$$\mathcal{H}_\phi = \begin{bmatrix} \widehat{\phi}(-1) & \widehat{\phi}(-2) & \widehat{\phi}(-3) & \cdots \\ \widehat{\phi}(-2) & \widehat{\phi}(-3) & \widehat{\phi}(-4) & \cdots \\ \widehat{\phi}(-3) & \widehat{\phi}(-4) & \widehat{\phi}(-5) & \cdots \\ \vdots & \vdots & \vdots & \ddots \end{bmatrix}.$$

The operator norm is

$$\|\mathcal{H}_\phi\| := \sup\{\|\mathcal{H}_\phi h\|_\infty : h \in \bar{B}H^\infty(\mathbf{D})\}.$$

The essential norm is

$$\|\mathcal{H}_\phi\|_e := \inf\{\|\mathcal{H}_\phi - K\| : K \text{ is a compact operator}\}.$$

The following version of Nehari’s Theorem emphasizes existence and uniqueness of best approximations.

**THEOREM 5.1** (NEHARI [56; 45]). *If  $\phi \in L^\infty(\mathbf{T})$ , then  $\phi$  admits best approximations from  $H^\infty(\mathbf{D})$  as follows:*

- N-1:  $\|\phi - H^\infty(\mathbf{D})\|_\infty = \|\mathcal{H}_\phi\|$ .
- N-2:  $\|\phi - \{H^\infty(\mathbf{D}) + C(\mathbf{T})\}\|_\infty = \|\mathcal{H}_\phi\|_e$ .
- N-3: *If  $\|\mathcal{H}_\phi\|_e < \|\mathcal{H}_\phi\|$  then best approximations are unique.*

Thus, Nehari’s Theorem computes the distance from  $\phi$  to  $H^\infty(\mathbf{D})$  using the Hankel matrix. However, solving the matching problem with lumped circuits forces us to minimize from the disk algebra  $\mathcal{A}(\mathbf{D})$ . Because the disk algebra is a proper subset of  $H^\infty(\mathbf{D})$ , there always holds the inequality:

$$\|\phi - \mathcal{A}(\mathbf{D})\|_\infty \geq \|\phi - H^\infty(\mathbf{D})\|_\infty = \|\mathcal{H}_\phi\|.$$

Fortunately for our application, equality holds when  $\phi$  is continuous.

THEOREM 5.2 (Adapted from [39, pages 193–195], [33; 34]). *If  $\phi \in 1\dot{+}C_0(j\mathbb{R})$ ,*

$$\|\phi - \mathcal{A}_1(\mathbb{C}_+)\|_\infty = \|\phi - H^\infty(\mathbb{C}_+)\|_\infty$$

*and there is exactly one  $h \in H^\infty(\mathbb{C}_+)$  such that*

$$\|\phi - \mathcal{A}_1(\mathbb{C}_+)\|_\infty = |\phi(j\omega) - h(j\omega)| \quad \text{a.e.}$$

Thus, continuity forces unicity and characterizes the minimum by the *circularity of the error*  $\phi - h$ . To get existence in the disk algebra requires more than continuity. Let  $\phi : \mathbb{R} \rightarrow \mathbb{C}$  be periodic with period  $2\pi$ . The *modulus of continuity* of  $\phi$  is the function [18, page 71]:

$$\omega(\phi; t) := \sup\{|\phi(t_1) - \phi(t_2)| : t_1, t_2 \in \mathbb{R}, |t_1 - t_2| \leq t\}.$$

Let  $\Lambda_\alpha$  denote those functions that satisfy a *Lipschitz condition of order  $\alpha \in (0, 1]$* :

$$|\phi(t_1) - \phi(t_2)| \leq A|t_1 - t_2|^\alpha.$$

Let  $C^{n+\alpha}$  denote those functions with  $\phi^{(n)} \in \Lambda_\alpha$  [5]. Let  $C_\omega$  denote those functions that are *Dini-continuous*:

$$\int_0^\varepsilon \omega(\phi; t)t^{-1}dt < \infty,$$

for some  $\varepsilon > 0$ . A sufficient condition for a function  $\phi(t)$  to be Dini-continuous is that  $|\phi'(t)|$  be bounded [19, section IV.2]. Carleson & Jacobs have an amazing paper that addresses best approximation from the disk algebra [5]:

THEOREM 5.3 (CARLESON & JACOBS [5]). *If  $\phi \in L^\infty(\mathbf{T})$ , then there always exists a best approximation  $h \in H^\infty(\mathbf{D})$ :*

$$\|\phi - h\|_\infty = \|\phi - H^\infty(\mathbf{D})\|_\infty.$$

*If  $\phi \in C(\mathbf{T})$ , then the best approximation is unique. Moreover,*

- (A): *If  $\phi \in C_\omega$  then  $h \in C_\omega$ .*
- (B): *If  $\phi^{(n)} \in C_\omega$  then  $h^{(n)} \in C_\omega$ .*
- (C): *If  $0 < \alpha < 1$  and  $\phi \in \Lambda_\alpha$  then  $h \in \Lambda_\alpha$ .*
- (D): *If  $0 < \alpha < 1$ ,  $n \in \mathbb{N}$ , and  $\phi \in C^{n+\alpha}$  then  $h \in C^{n+\alpha}$ .*

As noted by Carleson & Jacobs [5]: “the function-theoretic proofs ... are all of a local character, and so all the results can easily be carried over to any region which has in each case a sufficiently regular boundary.” Provided we can guarantee smoothness across  $\pm j\infty$ , Theorem 5.3 carries over to the right half-plane.

COROLLARY 5.1. *If  $\phi \in 1\dot{+}C_0(j\mathbb{R})$ , then the best approximation*

$$\|\phi - h\|_\infty = \|\phi - H^\infty(\mathbb{C}_+)\|_\infty$$

exists and is unique. Moreover, if  $\phi \circ \mathbf{c}^{-1} \in C_\omega$ , then  $h \circ \mathbf{c}^{-1} \in C_\omega$  so that

$$\|\phi - h\|_\infty = \|\phi - H^\infty(\mathbb{C}_+)\|_\infty = \|\phi - \mathcal{A}_1(\mathbb{C}_+)\|_\infty.$$

Thus, the smoothness of the target function  $\phi$  is invariant under the *best approximation operator* of  $H^\infty$ .

**5.2. Nonlinear Nehari and simple matching bounds.** Helton [28; 31; 29; 32] is extending Nehari's Theorem into a general Theory of Analytic Optimization. Let  $\Gamma : j\mathbb{R} \times \mathbb{C} \rightarrow \mathbb{R}_+ \cup \infty$  be continuous. Define  $\gamma : L^\infty(j\mathbb{R}) \rightarrow \mathbb{R}_+ \cup \infty$  by

$$\gamma(h) := \text{ess.sup}\{\Gamma(j\omega, h(j\omega)) : \omega \in \mathbb{R}\}.$$

and consider the minimization of  $\gamma$  on  $K \subseteq L^\infty(j\mathbb{R})$ :

$$\min\{\gamma(\phi) : \phi \in K\}.$$

Helton observed that many interesting problems in electrical engineering and control theory have the form of this minimization problem and furthermore in many cases the objective functions have sublevel sets that are disks [32]:

$$[\gamma \leq \alpha] := \{\phi \in \bar{B}L^\infty(j\mathbb{R}) : \gamma(\phi) \leq \alpha\} = \bar{D}(c_\alpha, r_\alpha).$$

This is certainly the case for the matching problem. For a given load  $s_L \in BL^\infty(j\mathbb{R})$ , we want to minimize the worst case mismatch

$$\gamma(s_2) = \Delta\rho(s_2) := \text{ess.sup}\{\Delta P(s_2(j\omega), s_L(j\omega)) : \omega \in \mathbb{R}\}$$

over all  $s_2 \in \bar{B}H^\infty(\mathbb{C}_+)$ . In this special case, Lemma 4.5 shows explicitly that the sublevel sets of  $\Delta\rho$  are disks. These sublevel sets govern the optimization problem. For a start, the sublevel sets determine the existence of minimizers.

LEMMA 5.1. *Let  $\gamma : \bar{B}L^\infty(j\mathbb{R}) \rightarrow \mathbb{R}$ . Assume  $\gamma$  has sublevel sets that are disks contained in  $\bar{B}L^\infty(j\mathbb{R})$ :*

$$[\gamma \leq \alpha] = \bar{D}(c_\alpha, r_\alpha) \subseteq \bar{B}L^\infty(j\mathbb{R}).$$

*Then  $\gamma$  has a minimizer  $h_{\min} \in \bar{B}H^\infty(\mathbb{C}_+)$ .*

PROOF. Lemma 3.2 gives that  $\gamma$  is lower semicontinuous in the weak-\* topology. Because  $\bar{B}H^\infty(\mathbb{C}_+)$  is weak-\* compact, the Weierstrass Theorem of Section 4.10 forces the existence of  $H^\infty$  minimizers.  $\square$

In particular, an  $H^\infty$  minimizer of power mismatch does exist. This is only the beginning; we'll see that the disk structure of the sublevel sets also couples with Nehari's Theorem to characterize such minimizers using Helton's fundamental link between disks and operators. Ultimately, this line of inquiry permits us to *calculate* the matching performance for real problems.

THEOREM 5.4 (HELTON [29, Theorem 4.2]). *Let  $C, P, R \in L^\infty(\mathbf{T}, \mathbb{C}^{N \times N})$ . Assume  $P$  and  $R$  are uniformly strictly positive. Define the disk*

$$\bar{D}(C, R, P) := \{\Phi \in L^\infty(\mathbf{T}, \mathbb{C}^{N \times N}) : (\Phi - C)P^2(\Phi - C)^H \leq R^2\}$$

and  $\check{R}(j\omega) := R(-j\omega)$ . Then

$$\emptyset \neq \bar{D}(C, R, P) \cap H^\infty(\mathbf{D}, \mathbb{C}^{N \times N}) \iff \mathcal{H}_C \mathcal{J}_{P^{-2}}^{-1} \mathcal{H}_C^* \leq \mathcal{J}_{\check{R}^2},$$

For the impedance matching problem,  $\gamma$  is the power mismatch  $\Delta P$  whose sublevel sets are contained in  $\bar{B}L^\infty(j\mathbb{R})$ :

$$\bar{D}(c_\alpha, r_\alpha) \cap \bar{B}H^\infty(\mathbb{C}_+) = \bar{D}(c_\alpha, r_\alpha) \cap H^\infty(\mathbb{C}_+).$$

Consequently, in our problem the unit ball constraint may be ignored and we may apply Theorem 5.4 specialized to the disk theory under this stronger assumption.

COROLLARY 5.2. *Let  $\gamma : \bar{B}L^\infty(j\mathbb{R}) \rightarrow \mathbb{R}$ . Assume  $\gamma$  has sublevel sets that are disks:*

$$[\gamma \leq \alpha] = \bar{D}(c_\alpha, r_\alpha) \subseteq \bar{B}L^\infty(j\mathbb{R}).$$

Let  $C_\alpha := c_\alpha \circ \mathbf{c}^{-1}$  and  $R_\alpha = r_\alpha \circ \mathbf{c}^{-1}$  where  $\mathbf{c}$  is the Cayley transform of Lemma 3.3. Assume  $R_\alpha$  is strictly uniformly positive with spectral factor  $Q_\alpha \in H^\infty(\mathbf{D})$ :  $R_\alpha = |Q_\alpha|$ . Then the following are equivalent:

- (A):  $\bar{D}(c_\alpha, r_\alpha) \cap \bar{B}H^\infty(\mathbb{C}_+) \neq \emptyset$
- (B):  $\mathcal{H}_{C_\alpha} \mathcal{H}_{C_\alpha}^* \leq \mathcal{J}_{\check{R}_\alpha^2}$
- (C):  $\|Q_\alpha^{-1} C_\alpha - H^\infty(\mathbf{D})\|_\infty \leq 1$ .

PROOF. By Theorem 5.4, all that is needed is to prove (a)  $\iff$  (c). If (a) is true, there exists an  $H \in \bar{B}H^\infty(\mathbf{D})$  such that  $|H - C_\alpha| \leq R_\alpha = |Q_\alpha|$  a.e. Because  $R_\alpha$  is strictly uniformly positive on  $\mathbf{T}$ , we may divide by  $|Q_\alpha|$  to get  $|Q_\alpha^{-1}H - Q_\alpha^{-1}C_\alpha| \leq 1$  a.e. Because  $Q_\alpha$  is outer,  $Q_\alpha^{-1}H \in H^\infty(\mathbf{D})$  so that (c) must be true. Conversely, suppose (c) is true. Because  $Q_\alpha$  is outer,  $Q_\alpha^{-1}C_\alpha \in L^\infty(j\mathbb{R})$ . The Cayley transform of Nehari's Theorem forces the existence of a  $G \in H^\infty(\mathbf{D})$  such that  $\|G - Q_\alpha^{-1}C_\alpha\|_\infty \leq 1$ . Because  $Q_\alpha$  is outer,  $H = Q_\alpha G \in H^\infty(\mathbf{D})$  and  $|H - C_\alpha| \leq R_\alpha$  a.e. Then  $H \in \bar{D}(C_\alpha, R_\alpha) \cap H^\infty(\mathbf{D})$ . Because  $\bar{D}(C_\alpha, R_\alpha)$  is assumed to be contained in the unit ball of  $L^\infty(\mathbf{T})$ , the Cayley transform forces (a) to hold.  $\square$

Part (b) amounts to an eigenvalue test that admits a nice graphical display of the minimizing  $\alpha$ . Let  $\lambda_{\inf}(\alpha)$  denote the smallest "eigenvalue" of  $\mathcal{J}_{\check{R}_\alpha^2} - \mathcal{H}_{C_\alpha} \mathcal{H}_{C_\alpha}^*$ . A plot of  $\alpha$  versus  $\lambda_{\inf}(\alpha)$  reveals that  $\lambda_{\inf}(\alpha)$  is a decreasing function of  $\alpha$  that crosses zero at a minimum. The next result verifies this assertion regarding the minimum.

COROLLARY 5.3. *Let  $\gamma : \bar{B}L^\infty(j\mathbb{R}) \rightarrow \mathbb{R}$ . Assume  $\gamma$  has sublevel sets that are disks contained in  $\bar{B}L^\infty(j\mathbb{R})$ :*

$$[\gamma \leq \alpha] = \bar{D}(c_\alpha, r_\alpha) \subseteq \bar{B}L^\infty(j\mathbb{R}).$$

Then  $\gamma$  has a minimizer  $h_{\min} \in \bar{B}H^\infty(\mathbb{C}_+)$ :

$$\gamma_{\bar{B}H^\infty} := \min\{\gamma(h) : h \in \bar{B}H^\infty(\mathbb{C}_+)\}.$$

Let  $c_{\min}$  and  $r_{\min}$  denote the  $L^\infty(j\mathbb{R})$  center and radius functions of the sublevel disk at the minimum level:  $[\gamma \leq \gamma_{\bar{B}H^\infty}]$ . Let  $C_\alpha := c_\alpha \circ \mathbf{c}^{-1}$  and  $R_\alpha = r_\alpha \circ \mathbf{c}^{-1}$  where  $\mathbf{c}$  is the Cayley transform of Lemma 3.3. Assume  $R_{\min}$  is strictly uniformly positive with spectral factor  $Q_{\min}$ . Then the following are equivalent:

MIN-1:  $\bar{D}(c_{\min}, r_{\min}) \cap \bar{B}H^\infty \neq \emptyset$

MIN-2:  $0 = \lambda_{\inf}(\gamma_{\bar{B}H^\infty})$

MIN-3:  $\|Q_{\min}^{-1}C_{\min} - H^\infty(\mathbf{D})\|_\infty = 1$ .

Moreover, if  $Q_{\min}^{-1}C_{\min} \in C(\mathbf{T})$  the minimizer  $h_{\min}$  is unique.

PROOF. Min-1  $\implies$  Min-3: If the inequality were strict,  $|C_{\min} - H| < R_{\min}$  a.e. for some  $H \in H^\infty(\mathbf{D})$ . Then  $h = H \circ \mathbf{c}$  belongs to  $H^\infty(\mathbb{C}_+)$  and drops  $\gamma$  below its minimum:  $\gamma(h) < \alpha_{\min}$ . This contradiction forces equality at the minimum. Min-3  $\implies$  Min-1: Corollary 5.2.

Min-1  $\implies$  Min-2: Theorem 5.4 forces  $\mathcal{H}_{C_{\min}} \mathcal{H}_{C_{\min}}^* \leq \mathcal{J}_{R_{\min}^2}$  or  $0 \leq \lambda_{\inf}(\gamma_{\bar{B}H^\infty})$ .

This operator inequality is equivalent to  $1 \geq \|\mathcal{H}_{Q_{\min}^{-1}C_{\min}}\|$  [29, page 42]. By Nehari's Theorem,  $1 \geq \|\mathcal{H}_{Q_{\min}^{-1}C_{\min}}\| = \|Q_{\min}^{-1}C_{\min} - H^\infty(\mathbf{D})\|_\infty = 1$ , where the equivalence of Min-1 and Min-3 gives the last equality. Thus, the inequality must be an equality. Min-2  $\implies$  Min-1:  $0 = \lambda_{\inf}(\gamma_{\bar{B}H^\infty})$  forces  $1 = \|\mathcal{H}_{Q_{\min}^{-1}C_{\min}}\|$ . By Nehari's Theorem,  $1 = \|Q_{\min}^{-1}C_{\min} - H^\infty(\mathbf{D})\|_\infty$ . The Cayley transform of Nehari's Theorem gives an  $H \in H^\infty(\mathbf{D})$  such that  $1 = \|Q_{\min}^{-1}C_{\min} - H\|_\infty$ . Multiply by the spectral factor to get  $R_{\min} = |C_{\min} - Q_{\min}H|$  or that  $\bar{D}(C_{\min}, R_{\min}) \cap H^\infty(\mathbf{D}) \neq \emptyset$ . Use the assumption that the sublevel sets are contained in the close unit ball to get Min-1. For unicity, Min-3 forces  $H_{\min} = h_{\min} \circ \mathbf{c}^{-1}$  to be a minimizer of  $1 = \|Q_{\min}^{-1}C_{\min} - H^\infty(\mathbf{D})\|_\infty = \|Q_{\min}^{-1}C_{\min} - H_{\min}\|_\infty$ . Because  $Q_{\min}^{-1}C_{\min}$  is continuous, the Cayley transform of Corollary 5.1 forces unicity.  $\square$

Lumped matching circuits have continuous scattering matrices. This requires us to constrain our minimization of power mismatch yet further to the disk algebra. For minimization of a general  $\gamma$  over the disk algebra, we always have

$$\gamma_{\bar{B}H^\infty} \leq \gamma_{\bar{B}A_1} := \inf\{\gamma(h) : h \in \bar{B}A_1(\mathbb{C}_+)\}.$$

Under smoothness and continuity conditions, equality between the disk algebra and  $H^\infty$  can be established.

COROLLARY 5.4. *In addition to the assumptions of Corollary 5.3, assume  $Q_{\min}^{-1}C_{\min}$  is Dini-continuous. Then*

$$\gamma_{\bar{B}H^\infty} = \gamma_{\bar{B}A_1} = \min\{\gamma(h) : h \in \bar{B}A_1(\mathbb{C}_+)\}.$$

PROOF. By Corollary 5.3, there is a unique minimizer  $H_{\min} \in H^\infty(\mathbf{D})$

$$1 = \|Q_{\min}^{-1} C_{\min} - H^\infty(\mathbf{D})\|_\infty = \|Q_{\min}^{-1} C_{\min} - H_{\min}\|_\infty.$$

By Corollary 5.1, Dini-continuity forces  $H_{\min}$  to be Dini-continuous or  $h_{\min} = H \circ \mathbf{c} \in \mathcal{A}_1(\mathbb{C}_+)$ . Thus, the inclusion of the  $H^\infty$  minimizer in the disk algebra forces  $\gamma_{\bar{B}H^\infty} = \gamma_{\bar{B}\mathcal{A}_1}$ .  $\square$

This is a useful general result, but for our matching problem the requirement of Dini-continuity can in fact be relaxed. An easier approach, specialized to the case of  $\gamma$  is the power mismatch, gives equality between the minimum over the disk algebra and that over  $H^\infty$  using only continuity (proof in Appendix D).

THEOREM 5.5. *Assume  $s_L \in \mathcal{BA}_1(\mathbb{C}_+)$ . Then*

$$\inf\{\|\Delta P(s_2, s_L)\|_\infty : s_2 \in \bar{B}H^\infty(\mathbb{C}_+)\} = \inf\{\|\Delta P(s_2, s_L)\|_\infty : s_2 \in \bar{B}\mathcal{A}_1(\mathbb{C}_+)\}.$$

**5.3. The real constraint.** Examination of the circuits in Section 4 shows the scattering matrices are real:  $S(p) = \overline{S(\bar{p})}$ . In fact, the scattering matrices that are used in the matching problem must satisfy this *real constraint*. Those  $H^\infty$  functions satisfying this real constraint form a proper subset  $\text{Re } H^\infty(\mathbb{C}_+)$ , which generally forces the inequality:

$$\inf\{\|\phi - h\|_\infty : h \in \text{Re } H^\infty(\mathbb{C}_+)\} \geq \|\phi - H^\infty(\mathbb{C}_+)\|_\infty$$

However, equality is obtained provided  $\phi$  is also real. That the best approximation operator preserves the real constraint is an excellent illustration of the general principle: That the best approximation operator preserves symmetries.

LEMMA 5.2. *Let  $(\mathcal{X}, d)$  be a metric space. Assume  $A : \mathcal{X} \rightarrow \mathcal{X}$  is a contractive map:  $d(A(x), A(y)) \leq d(x, y)$ . Let  $\mathcal{V} \subseteq \mathcal{X}$  be nonempty. Define  $\text{dist}(x, \mathcal{V}) := \inf\{d(x, v) : v \in \mathcal{V}\}$ . Assume*

A-1:  $\mathcal{V}$  is  $A$ -invariant:  $A(\mathcal{V}) \subseteq \mathcal{V}$ .

A-2:  $x \in \mathcal{X}$  is also  $A$ -invariant  $A(x) = x$ .

*Then equality holds:  $\text{dist}(x, A(\mathcal{V})) = \text{dist}(x, \mathcal{V})$ .*

PROOF. Let  $\{v_n\}$  be a minimizing sequence:  $d(x, v_n) \rightarrow \text{dist}(x, \mathcal{V})$ . Because  $x$  is  $A$ -invariant,  $d(x, A(v_n)) = d(A(x), A(v_n)) \leq d(x, v_n) \rightarrow \text{dist}(x, \mathcal{V})$ . Thus,  $\text{dist}(x, A(\mathcal{V})) \leq \text{dist}(x, \mathcal{V})$  forces equality.  $\square$

Lemma 5.2 makes explicit the structure to handle the real constraint in the matching problem.

COROLLARY 5.5. *If  $s_L \in B \text{Re } L^\infty(j\mathbb{R})$ , there holds*

$$\inf\{\|\Delta P(s_2, s_L)\|_\infty : s_2 \in \bar{B}\mathcal{A}_1(\mathbb{C}_+)\} = \inf\{\|\Delta P(s_2, s_L)\|_\infty : s_2 \in \text{Re } \bar{B}\mathcal{A}_1(\mathbb{C}_+)\}.$$

PROOF. Apply Lemma 5.2 identifying  $BL^\infty(j\mathbb{R})$  as the metric space,  $\tilde{\phi}(j\omega) = \overline{\phi(j\omega)}$  as the contraction,  $\text{Re } BA_1(\mathbb{C}_+)$  as the  $\tilde{\sim}$ -invariant subset, and  $s_L$  as the  $\tilde{\sim}$ -invariant target function. Recall that the power mismatch  $\Delta P(s_2, s_L)$  is the pseudohyperbolic metric  $\rho(\overline{s_2}, s_L)$  (Section 4.8). Because  $\rho$  is a metric, it follows that  $\|\rho\|_\infty$  is also metric that is  $\tilde{\sim}$ -invariant:  $\|\rho(\tilde{s}_2, \tilde{s}_L)\|_\infty = \|\rho(s_2, s_L)\|_\infty$ . The technical complication is that  $\Delta P(s_2, s_L)$  is well-defined only when one of its arguments is restricted to the open unit ball  $BL^\infty(j\mathbb{R})$ . With  $s_L \in B\text{Re } L^\infty(j\mathbb{R})$ , Lemma 4.6 asserts that  $s_2 \mapsto \|\Delta P(s_2, s_L)\|_\infty$  is a continuous mapping on  $\overline{BL^\infty}(j\mathbb{R})$ . Thus, we use continuity to drop the  $\overline{B}$  constraint, apply Lemma 5.2 to the open ball with the real contraction “ $\tilde{\sim}$ ”, and apply continuity again to close the open ball:

$$\begin{aligned} \inf\{\|\Delta P(s_2, s_L)\|_\infty : s_2 \in \text{Re } \overline{BA}_1(\mathbb{C}_+)\} \\ &\stackrel{\text{Lemma 4.6}}{=} \inf\{\|\Delta P(s_2, s_L)\|_\infty : s_2 \in \text{Re } BA_1(\mathbb{C}_+)\} \\ &\stackrel{\text{Eq. 4-10}}{=} \inf\{\|\rho(\overline{s_2}, s_L)\|_\infty : s_2 \in \text{Re } BA_1(\mathbb{C}_+)\} \\ &\stackrel{\text{Corollary 5.5}}{=} \inf\{\|\rho(\overline{s_2}, s_L)\|_\infty : s_2 \in BA_1(\mathbb{C}_+)\} \\ &\stackrel{\text{Eq. 4-10}}{=} \inf\{\|\Delta P(s_2, s_L)\|_\infty : s_2 \in BA_1(\mathbb{C}_+)\} \\ &\stackrel{\text{Lemma 4.6}}{=} \inf\{\|\Delta P(s_2, s_L)\|_\infty : s_2 \in \overline{BA}_1(\mathbb{C}_+)\}. \quad \square \end{aligned}$$

Not surprisingly, Helton has also uncovered another notion of “real-invariance” for general nonlinear minimization [32].

## 6. Classes of Lossless 2-Ports

The matching problems are optimization problems over classes of  $U^+(2)$ :

$$U^+(2, d) \subset U^+(2, \infty) \subset U^+(2) \subset \text{Re } \overline{BH}^\infty(\mathbb{C}_+, \mathbb{C}^{2 \times 2}).$$

On the left,  $U^+(2, d)$  corresponds to the lumped, lossless 2-ports. Optimization over this set represents an electrical engineering solution. On the right, the  $H^\infty$  solution provided in the last section is computable from the measured data but may not correspond to any lossless scattering matrix. The gap between the  $H^\infty$  solution and the various electrical engineering solutions may be closed by continuity conditions.

The first result on gives the correspondence between the lumped  $N$ -ports and their scattering matrices.

THE CIRCUIT-SCATTERING CORRESPONDENCE [52, Theorems 3.1, 3.2]. *Any  $N$ -port composed of a finite number of lumped elements (positive resistors, capacitors, inductors, transformers, gyrators) admits a real, rational, lossless scattering matrix  $S \in U^+(N)$ . Conversely, to any real, rational, scattering matrix  $S \in U^+(N)$  there corresponds an  $N$ -port composed of a finite number of lumped elements*

This equivalence permits us to delineate the following class of lossless 2-ports by their scattering matrices:

$$U^+(2, d) := \{S \in U^+(2) : \deg_{\text{SM}}[S(p)] \leq d\},$$

where  $\deg_{\text{SM}}[S(p)]$  denotes the Smith–McMillan degree (defined in Theorem 6.2). The second result establishes compactness (Appendix C contains the proof).

**THEOREM 6.1.** *Let  $d \geq 0$ .  $U^+(N, d)$  is a compact subset of  $\mathcal{A}_1(\mathbb{C}_+, \mathbb{C}^{N \times N})$ .*

It is straight-forward but tedious to demonstrate that the gain function  $S \mapsto \|G_T(s_G, S, s_L)\|_{-\infty}$  is a continuous function on  $U^+(2, d)$ . Thus, the matching problem on  $U^+(2, d)$  has a solution. The third result on  $U^+(2, d)$  is the Belevitch parameterization.

**BELEVITCH'S THEOREM [53]**  $S \in U^+(2, d)$  if and only if

$$S(p) = \begin{bmatrix} s_{11}(p) & s_{12}(p) \\ s_{21}(p) & s_{22}(p) \end{bmatrix} = \frac{1}{g(p)} \begin{bmatrix} h(p) & f(p) \\ \pm f_*(p) & \mp h_*(p) \end{bmatrix},$$

where  $f_*(p) := f(-p)$  and

B-1:  $f(p)$ ,  $g(p)$ , and  $h(p)$  are real polynomials,

B-2:  $g(p)$  is strict Hurwitz<sup>5</sup> of degree not exceeding  $d$ ,

B-3:  $g_*(p)g(p) = f_*(p)f(p) + h_*(p)h(p)$  for all  $p \in \mathbb{C}$ .

Belevitch's Theorem lets us characterize several classes of 2-ports, such as the low-pass and high-pass ladders. The low-pass ladders (Figure 11) admit the scattering matrix characterization [3, page 121]:

$$s_{21}(p) = \frac{1}{g(p)}.$$

These scattering matrices ( $f(p) = 1$ ) form a closed and therefore compact subset of  $U^+(2, d)$ . Consequently, the matching problem admits a solution over the class of low-pass ladders. Figure 17 shows a high-pass ladder. A high-pass ladder admits the scattering matrix characterization [3, page 122]:

$$s_{21}(p) = \frac{p^{\partial g}}{g(p)},$$

where  $\partial g$  denotes the degree of the polynomial  $g(p)$ . The high-pass ladders form

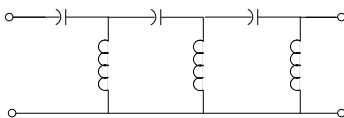


**Figure 17.** A high-pass ladder.

<sup>5</sup>The zeros of  $g(p)$  lie in the open left half-plane.

a closed and therefore compact subset of  $U^+(2, d)$ . Consequently, the matching problem admits a solution over the class of high-pass ladders.

The fourth result on  $U^+(2, d)$  is the state-space parameterization illustrated in Figure 18. The  $N$ -port has a scattering matrix  $S \in U^+(N, d)$ , where  $d = \deg_{\text{SM}}[S(p)]$  counts the number of inductors and capacitors. The figure shows that by pulling all the  $d$  reactive elements into the *augmented load*  $S_L(p)$ . What's left is an  $(N + d)$ -port with a *constant* scattering matrix  $S_a$  called the *augmented scattering* matrix. Then  $S_a$  models the  $(N + d)$ -port as a collection of wires, transformers, and gyrators. Consequently,  $S_a$  is a real, unitary, and *constant* matrix. Thus,  $S(p)$  is the image of the augmented load viewed through the augmented scattering matrix. Theorem 6.2 gives the precise statement of this *state-space representation*.

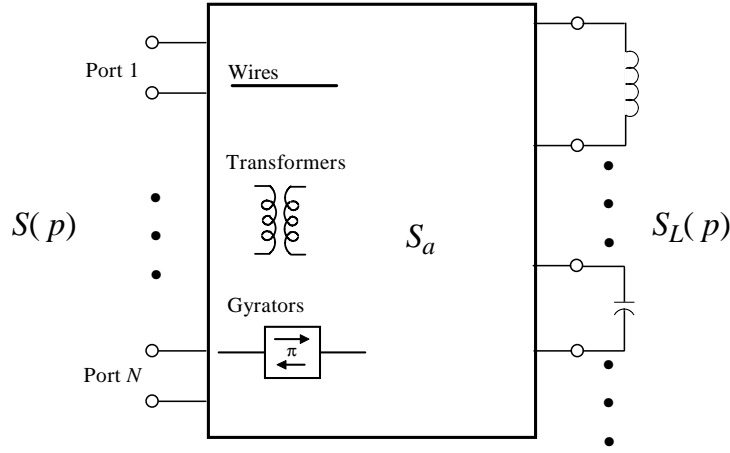


**Figure 18.** State-space representation of a lumped, lossless  $N$ -port containing  $d$  reactive elements.

**THEOREM 6.2 (STATE-SPACE [52, pages 90–93]).** *Every lumped, lossless, casual, time-invariant  $N$ -port admits a scattering matrix  $S(p)$  and conversely. If  $S(p)$  has degree  $d$ ,  $S(p)$  admits the following state-space representation:*

$$S(p) = \mathcal{F}(S_a, S_L; p) := S_{a,11} + S_{a,12}S_L(p)(I_d - S_{a,22}S_L)^{-1}S_{a,21},$$

where the augmented load is

$$S_L(p) = \frac{p-1}{p+1} \begin{bmatrix} I_{N_L} & 0 \\ 0 & -I_{N_C} \end{bmatrix}$$

and  $N_L + N_C = d$  counts the number of inductors and capacitors. The augmented scattering matrix is

$$S_a = \begin{bmatrix} S_{a,11} & S_{a,12} \\ S_{a,21} & S_{a,22} \end{bmatrix} \begin{matrix} N \\ d \\ N \quad d \end{matrix}$$

is a constant, real, orthogonal matrix.

This representation reveals the structure of the lumped, lossless  $N$ -ports, offers a numerically efficient parameterization of  $U^+(N, d)$  in terms of the orthogonal group, proves the Circuit-Scattering Correspondence, generalizes to lumped, passive  $N$ -ports, and provides an approach to non-lumped or distributed  $N$ -ports.

A natural generalization drops the constraint on the number of reactive elements in the 2-port and asks: *What is the matching set that is obtained as  $\deg_{\text{SM}}[S(p)] \rightarrow \infty$ ?* Define

$$U^+(2, \infty) = \bigcup_{d \geq 0} \overline{U^+(2, d)}.$$

The physical meaning of  $U^+(2, \infty)$  is that it contains the scattering matrices of all lumped, lossless 2-ports. It is worthwhile to ask: *Has the closure has picked up additional circuits?* Mathematically, a lossless matching  $N$ -port has a scattering matrix  $S(p)$  that is a real inner function. Inner functions exhibit a fascinating behavior at the boundary. For example, inner functions can interpolate a sequence of closed, connected subsets  $K_m \subseteq \overline{\mathbf{D}}$  [12]:  $\lim_{r \rightarrow 1} S(re^{j\theta_m}) = K_m$ . In contrast to this boundary behavior, if the lossless  $N$ -port is lumped, then  $S$  is rational and so must continuous. The converse is true and demonstrated in Appendix A.

**COROLLARY 6.1.** *Let  $S \in H^\infty(\mathbb{C}_+, \mathbb{C}^{N \times N})$  be an inner function. The following are equivalent:*

(A):  $S \in \mathcal{A}_1(\mathbb{C}_+, \mathbb{C}^{N \times N})$ .

(B):  $S$  is rational

Corollary 6.1 answers our question above with the negative:

$$U^+(2, \infty) = \bigcup_{d \geq 0} U^+(2, d).$$

Thus, continuity forces  $S \in U^+(2, \infty)$  to be rational and the corresponding lossless 2-port to be lumped. It is natural to ask: *What lossless 2-ports are not in  $U^+(2, \infty)$ ?*

**EXAMPLE 6.1 (TRANSMISSION LINE).** A uniform, lossless transmission line of characteristic impedance  $Z_c$  and *commensurate* length  $l$  is called a unit element (UE) with chain matrix [3, Equation 8.1]

$$\begin{bmatrix} v_1 \\ i_1 \end{bmatrix} = \begin{bmatrix} \cosh(\tau p) & Z_c \sinh(\tau p) \\ Y_c \sinh(\tau p) & \cosh(\tau p) \end{bmatrix} \begin{bmatrix} v_2 \\ -i_2 \end{bmatrix},$$

where  $\tau$  is the commensurate one-way delay  $\tau = l/c$  determined by the speed of propagation  $c$ .

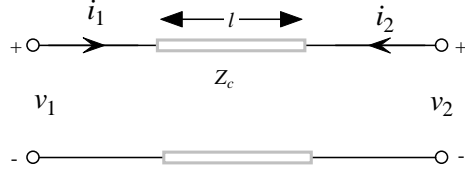


**Figure 19.** The unit element (UE) transmission line.

The scattering matrix of the transmission line **normalized to  $Z_c$**  is

$$S_{\text{UE}}(p) = \begin{bmatrix} 0 & e^{-\tau p} \\ e^{-\tau p} & 0 \end{bmatrix}$$

and gives rise to two observations: First,  $S_{\text{UE}}(j\omega)$  oscillates out to  $\pm\infty$ , so  $S_{\text{UE}}(j\omega)$  cannot be continuous across  $\pm\infty$ . Thus,  $U^+(2, \infty)$  cannot contain such a transmission line. Second, a physical transmission line cannot behave like this near  $\pm\infty$ . Many electrical engineering books mention only in passing that their models are applicable only for a given frequency band. One rarely sees much discussion that the models for the inductor and capacitor are essentially low-frequency models. This holds true even for the standard model of wire. One cannot shine a light in one end of a 100-foot length of copper wire and expect much out of the other end. These model limitations notwithstanding, the circuit-scattering correspondence will be developed using these standard models. The transmission line on the disk is

$$S_{\text{UE}} \circ \mathbf{c}^{-1}(z) = \begin{bmatrix} 0 & \exp\left(-\tau \frac{1+z}{1-z}\right) \\ \exp\left(-\tau \frac{1+z}{1-z}\right) & 0 \end{bmatrix}$$

and is recognizable as the simplest singular inner function [35, pages 66–67] analytic on  $\mathbb{C} \setminus \{1\}$  [35, pages 68–69]. Figure 20 shows the essential singularity of the real part of the (1,2) element of  $S_{\text{UE}} \circ \mathbf{c}^{-1}(z)$  as  $z$  tends toward the boundary of the unit circle.

## 7. Orbits and Tight Bounds for Matching

The following equalities convert a 2-port problem into a 1-port problem. Let  $\mathcal{U}$  be a subset of  $U^+(2)$ . Let

$$\mathcal{F}_1(\mathcal{U}, s_L) := \{\mathcal{F}_1(S, s_L) : S \in \mathcal{U}\}, \quad \mathcal{F}_2(\mathcal{U}, s_G) := \{\mathcal{F}_2(S, s_G) : S \in \mathcal{U}\}$$

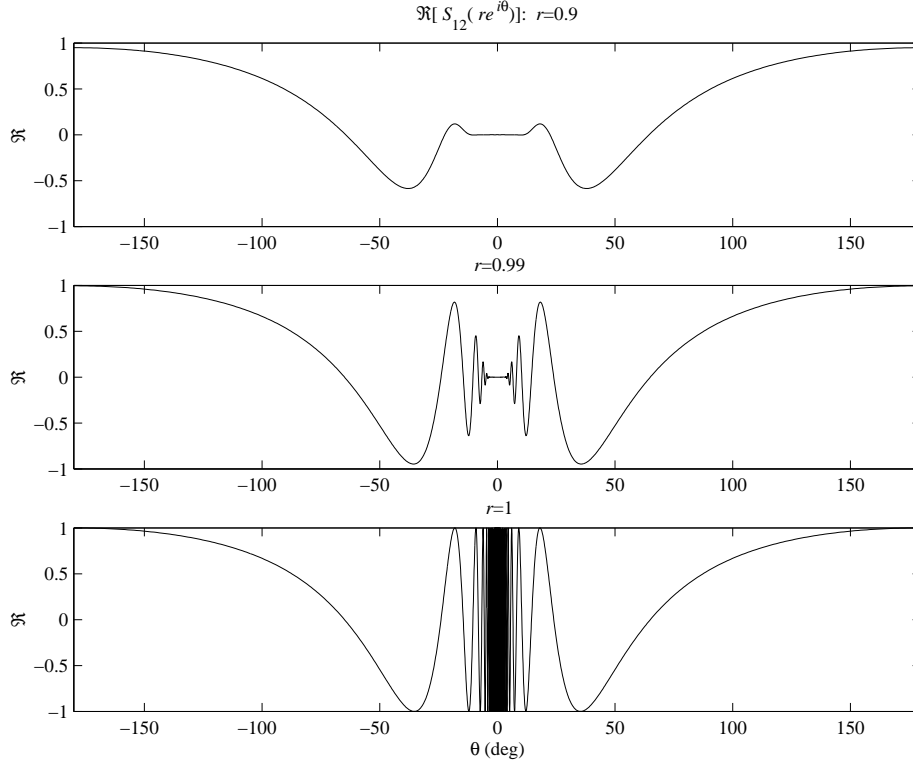


**Figure 20.** Behavior of  $\text{Re}[S_{\text{UE},12} \circ \mathbf{c}^{-1}(z)]$  for  $z = re^{j\theta}$  as  $r \rightarrow 1$ .

denote the orbit of the load and the orbit of the generator, respectively. By Lemma 4.4,

$$\begin{aligned} \sup\{\|G_T(s_G, S, s_L)\|_{-\infty} : S \in \mathcal{U}\} &= 1 - \inf\{\|\Delta P(s_G, S, s_L)\|_{\infty}^2 : S \in \mathcal{U}\} \\ &= 1 - \inf\{\|\Delta P(s_G, s_1)\|_{\infty}^2 : s_1 \in \mathcal{F}_1(\mathcal{U}; s_L)\} \\ &= 1 - \inf\{\|\Delta P(s_2, s_L)\|_{\infty}^2 : s_2 \in \mathcal{F}_2(\mathcal{U}; s_G)\}, \end{aligned}$$

or maximizing the gain on  $\mathcal{U}$  is equivalent to minimizing the power mismatch on either orbit. Darlington's Theorem makes explicit a class of orbits.

**THEOREM 7.1 (DARLINGTON [3]).** *The orbits of zero under the lumped, lossless 2-ports are equal*

$$\mathcal{F}_2(U^+(2, \infty), 0) = \mathcal{F}_1(U^+(2, \infty), 0)$$

and strictly dense in  $\text{Re } \bar{B}\mathcal{A}_1(\mathbb{C}_+)$ .

**PROOF.** Let  $S \in U^+(2, \infty)$ . Corollary 6.1 and Belevitch's Theorem give that

$$S(p) = \frac{1}{g} \begin{bmatrix} h & f \\ \pm f_* & \mp h_* \end{bmatrix} \in \text{Re } \mathcal{A}_1(\mathbb{C}_+, \mathbb{C}^{2 \times 2}),$$

where  $(f, g, h)$  is a Belevitch triple. With  $s_L = 0$  and  $s_G = 0$ , both  $s_1 = \mathcal{F}_1(S, 0) = h/g$  and belong to  $\text{Re } \bar{\mathcal{B}}\mathcal{A}_1(\mathbb{C}_+)$ . However, Corollary 6.1 restricts  $S$  to be rational so the orbits cannot be all of  $\text{Re } \bar{\mathcal{B}}\mathcal{A}_1(\mathbb{C}_+)$ . By relabeling  $S$  with  $1 \leftrightarrow 2$ , we get equality between the orbits. To show density, suppose  $s \in \text{Re } \bar{\mathcal{B}}\mathcal{A}_1(\mathbb{C}_+)$ . Because the rational functions in  $\text{Re } \bar{\mathcal{B}}\mathcal{A}_1(\mathbb{C}_+)$  are a dense<sup>6</sup> subset, we may approximate  $s(p)$  by a real rational function:  $s \approx h/g \in \text{Re } \bar{\mathcal{B}}\mathcal{A}_1(\mathbb{C}_+)$ , where  $h(p)$  and  $g(p)$  may be taken as real polynomials with  $g(p)$  strict Hurwitz and for all  $\omega \in \mathbb{R}$ :  $g(j\omega)g_*(j\omega) - h(j\omega)h_*(j\omega) \geq 0$ . By factoring  $g(p)g_*(p) - h(p)h_*(p)$  or appealing to the Fejér–Riesz Theorem [46, page 109], we can find a real polynomial  $f(p)$  such that

$$f(p)f_*(p) = g(p)g_*(p) - h(p)h_*(p).$$

The conditions of Belevitch's Theorem are met and

$$S(p) = \frac{1}{g(p)} \begin{bmatrix} h(p) & f(p) \\ f_*(p) & -h_*(p) \end{bmatrix}$$

is a lossless scattering matrix that represents a lumped, lossless 2-port. That is,  $h(p)/g(p)$  dilates to a lossless scattering matrix  $S(p)$  for which  $s \approx s_{11}$ . Consequently, both orbits are dense in  $\text{Re } \bar{\mathcal{B}}\mathcal{A}_1(\mathbb{C}_+)$ .  $\square$

At this point we are in position to obtain a tight bound on matching performance in the special case of vanishing generator reflectance,  $s_G = 0$ . For any given load  $s_L \in \bar{B}H^\infty(\mathbb{C}_+)$ . Lemma 4.6 shows that  $s_2 \mapsto \|\Delta P(s_2, s_L)\|_\infty$  is continuous. This continuity, coupled with the density claims of Darlington's Theorem, gives:

$$\begin{aligned} & \max\{G_T(0, S, s_L) : S \in U^+(2, d)\} \\ &= 1 - \min\{\|\Delta P(s_2, s_L)\|_\infty^2 : s_2 \in \mathcal{F}_2(U^+(2, d); 0)\} \\ &\leq 1 - \inf\{\|\Delta P(s_2, s_L)\|_\infty^2 : s_2 \in \mathcal{F}_2(U^+(2, \infty); 0)\} \\ &\stackrel{\text{Darlington}}{=} 1 - \inf\{\|\Delta P(s_2, s_L)\|_\infty^2 : s_2 \in \text{Re } \bar{\mathcal{B}}\mathcal{A}_1(\mathbb{C}_+)\} \\ &\leq 1 - \inf\{\|\Delta P(s_2, s_L)\|_\infty^2 : s_2 \in \bar{B}H^\infty(\mathbb{C}_+)\}. \end{aligned}$$

The “max” and the “min” are used because  $U^+(2, d)$  is compact (Theorem 6.1) and  $G_T$  is continuous. The last infimum is attained by a minimizer by the Weierstrass Theorem using the weak-\* compactness of  $\bar{B}H^\infty(\mathbb{C}_+)$  (page 10) and the weak-\* lower semicontinuity of the power mismatch (Section 4.10). The minimum can be computed using the Nonlinear Nehari Theorem (See the comments following Corollary 5.2 and Corollary 5.3). Thus, the impedance matching problem has a *computable* bound:

---

<sup>6</sup>Density claims on unbounded regions can be tricky. However, Lemma 3.3 isometrically maps  $\mathcal{A}_1(\mathbb{C}_+) = \mathcal{A}_1(\mathbf{D}) \circ \mathbf{c}$  and preserves the rational functions. Therefore, the dense rational functions in  $\mathcal{A}(\mathbf{D})$  map to a set of rational functions in  $\mathcal{A}_1(\mathbb{C}_+)$  that must be dense.

$$\begin{aligned}
& \max\{G_T(0, S, s_L) : S \in U^+(2, d)\} \\
&= 1 - \min\{\|\Delta P(s_2, s_L)\|_\infty^2 : s_2 \in \mathcal{F}_2(U^+(2, d); 0)\} \\
&\leq 1 - \inf\{\|\Delta P(s_2, s_L)\|_\infty^2 : s_2 \in \mathcal{F}_2(U^+(2, \infty); 0)\} \\
&\stackrel{\text{Darlington}}{=} 1 - \inf\{\|\Delta P(s_2, s_L)\|_\infty^2 : s_2 \in \text{Re } \bar{B}\mathcal{A}_1(\mathbb{C}_+)\} \\
&\leq 1 - \min_{\text{Corollary 5.3}} \{\|\Delta P(s_2, s_L)\|_\infty^2 : s_2 \in \bar{B}H^\infty(\mathbb{C}_+)\} \text{ (computable)}.
\end{aligned}$$

The real constraint can be relaxed for real loads  $s_L$  by Corollary 5.5:

$$\begin{aligned}
& \max\{G_T(0, S, s_L) : S \in U^+(2, d)\} \\
&= 1 - \min\{\|\Delta P(s_2, s_L)\|_\infty^2 : s_2 \in \mathcal{F}_2(U^+(2, d); 0)\} \\
&\leq 1 - \inf\{\|\Delta P(s_2, s_L)\|_\infty^2 : s_2 \in \mathcal{F}_2(U^+(2, \infty); 0)\} \\
&\stackrel{\text{Darlington}}{=} 1 - \inf\{\|\Delta P(s_2, s_L)\|_\infty^2 : s_2 \in \text{Re } \bar{B}\mathcal{A}_1(\mathbb{C}_+)\} \\
&\stackrel{\text{Corollary 5.5}}{=} 1 - \inf\{\|\Delta P(s_2, s_L)\|_\infty^2 : s_2 \in \bar{B}\mathcal{A}_1(\mathbb{C}_+)\} \\
&\leq 1 - \min_{\text{Corollary 5.3}} \{\|\Delta P(s_2, s_L)\|_\infty^2 : s_2 \in \bar{B}H^\infty(\mathbb{C}_+)\} \text{ (computable)}.
\end{aligned}$$

Finally, the last inequality is actually equality if  $s_L$  is sufficiently smooth, using Theorem 5.5. Rolling it all up, we see that  $s_L \in \text{Re } B\mathcal{A}_1(\mathbb{C}_+)$  forces a lot of equalities:

$$\begin{aligned}
& \max\{G_T(0, S, s_L) : S \in U^+(2, d)\} \\
&= 1 - \min\{\|\Delta P(s_2, s_L)\|_\infty^2 : s_2 \in \mathcal{F}_2(U^+(2, d); 0)\} \\
&\leq 1 - \inf\{\|\Delta P(s_2, s_L)\|_\infty^2 : s_2 \in \mathcal{F}_2(U^+(2, \infty); 0)\} \\
&\stackrel{\text{Darlington}}{=} 1 - \inf\{\|\Delta P(s_2, s_L)\|_\infty^2 : s_2 \in \text{Re } \bar{B}\mathcal{A}_1(\mathbb{C}_+)\} \\
&\stackrel{\text{Corollary 5.5}}{=} 1 - \inf\{\|\Delta P(s_2, s_L)\|_\infty^2 : s_2 \in \bar{B}\mathcal{A}_1(\mathbb{C}_+)\} \\
&\stackrel{\text{Theorem 5.5}}{=} 1 - \min_{\text{Corollary 5.3}} \{\|\Delta P(s_2, s_L)\|_\infty^2 : s_2 \in \bar{B}H^\infty(\mathbb{C}_+)\} \text{ (computable)}.
\end{aligned}$$

Physically, this tight Nehari bound means that a lossless 2-port can be found with smallest possible power mismatch and that there is a sequence of lumped, lossless 2-ports that can get arbitrarily close to this bound. Furthermore, this bound can be computed from measured data on the load.

## 8. Matching an HF Antenna

Recent measurements were acquired on the forward-mast integrated HF antenna on the LPD 17, an amphibious transport dock. The problem is match this

antenna over 9-30 MHz to a 50-ohm line impedance using the simplest matching circuit possible. The goal is to find a simple matching circuit that gets the smallest power mismatch or the smallest VSWR (Section 4.8) Thus, a practical matching problem is complicated by not only minimizing the VSWR but making a tradeoff between VSWR and circuit complexity.

We start with a transformer, consider low- and high-pass ladders, and then show how the Nehari bound benchmarks these matching efforts. The transformer has chain and chain scattering matrices parameterized by its turns ratio  $n$  (see [3, Eq. 2.4] and [25, Table 6.2]; see also Figure 4 and Equation 4-1):

$$T_{\text{transformer}} = \begin{bmatrix} n^{-1} & 0 \\ 0 & n \end{bmatrix} \quad \Theta_{\text{transformer}} = \frac{1}{2n} \begin{bmatrix} 1 + n^2 & 1 - n^2 \\ 1 - n^2 & 1 + n^2 \end{bmatrix}.$$

Figure 21 displays the power mismatch as a function of the turns ratio  $n$ . This optimal  $n$  produced Figure 5 in the introduction. The antenna's load  $s_L$  is plotted as the solid curve in the unit disk. The solid disk corresponds to those reflectances with VSWR less than 4. The dotted line plots the reflectance looking to Port 1 of the optimal transformer with Port 2 terminated in the antenna:  $s_1 = \mathcal{G}_1(\Theta_{\text{transformer}}, s_L)$ . Lemma 4.4 demonstrates that matching at either port is equivalent when the 2-port is lossless.

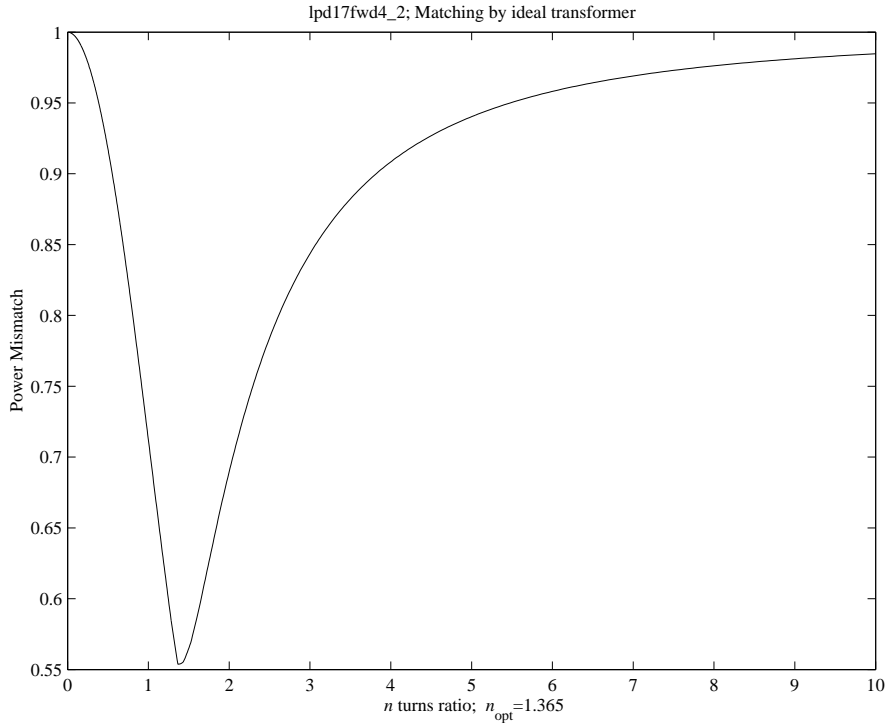
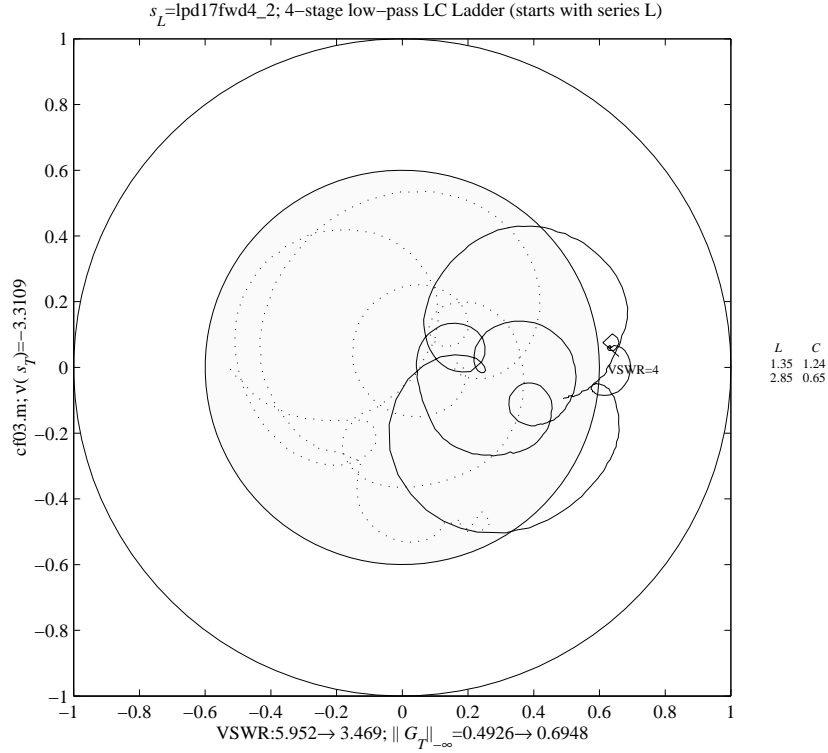


Figure 21. Power mismatch of an ideal transformer.



**Figure 22.** The antenna's reflectance  $s_L$  (solid) and the reflectance  $s_1$  after matching with a low-pass ladder of order 4.

Figure 22 matches the antenna with a low-pass ladder of order 4 (See Figure 11). Comparison with the transformer shows little is to be gained with the extra complexity. So it is very tempting to try longer ladders, or switch to high-pass ladders, or just start throwing circuits at the antenna. The first step to gain control over the matching processes is conduct a search over all lumped, lossless 2-port of degree not exceeding  $d$ :

$$d \mapsto \min\{\|\Delta P(\mathcal{F}_2(S, s_G), s_L)\|_\infty : S \in U^+(2, d)\}.$$

The state-space representation of Theorem 6.2 provides a numerically efficient parameterization of these lossless 2-ports. Figure 23 reports on matching from  $U^+(2, 4)$ . What is interesting is that  $s_2$  is starting to take a circular shape. This circular shape is no accident. Mathematically, Nehari's Theorem implies that the error is constant at optimum  $s_2$ :

$$\Delta P(s_2(j\omega), s_L(j\omega)) = \rho_{\min}.$$

The electrical engineers know the practical manifestation of Nehari's Theorem. For example, a broadband matching technique is described as follows [55]: The

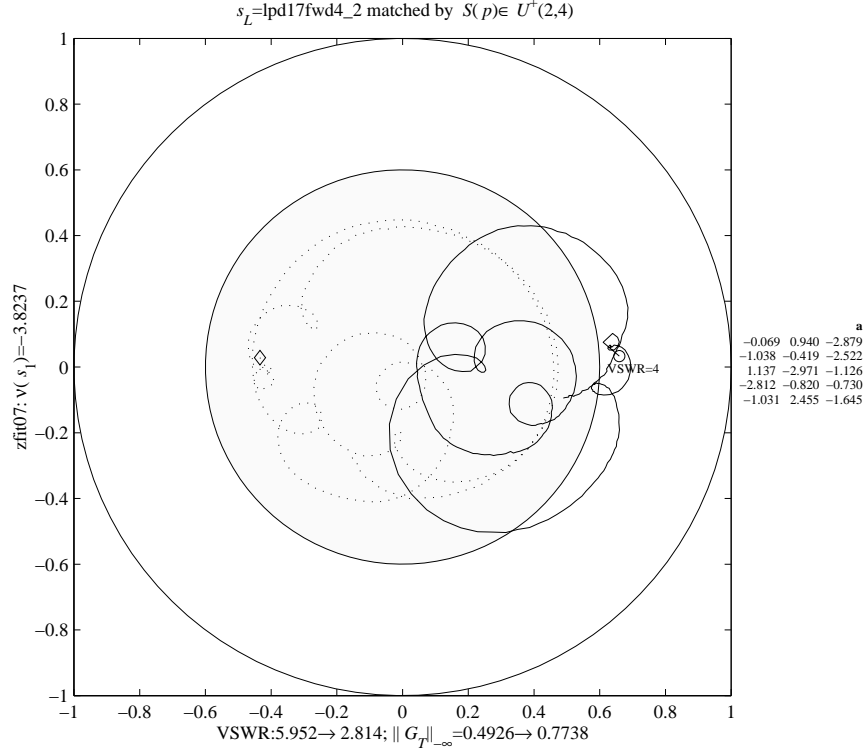


**Figure 23.** The antenna's reflectance  $s_L$  (solid) and the reflectance  $s_1$  after matching over  $U^+(2, 4)$ .

load impedance  $z_L$  is plotted in the Smith chart. The engineer is to terminate this load with a cascade of lossless two-ports. By repeatedly applying “shunt-stub/series-line cascades, a skilled designer using simulation software can see [the terminated impedance  $z_T$ ] form into a fairly tight circle around  $z = 1$ .” The appearance of a circle is a real-world demonstration that Nehari's Theorem is heuristically understood by microwave engineers.

The final step for bounding the matching process is to estimate the Nehari bound. Combine the eigenvalue test of Corollary 5.2 with the characterization of the power mismatch disks in Lemma 4.5: There is an  $s_2 \in \bar{B}H^\infty(\mathbb{C}_+)$  with

$$\|\Delta(s_2, s_L)\|_\infty \leq \rho \iff \mathcal{T}_{\bar{R}_\rho^2} \geq \mathcal{H}_{C_\rho} \mathcal{H}_{C_\rho}^*,$$

where the center and radius functions are

$$C_\rho = k_\rho \circ \mathbf{c}^{-1}, \quad k_\rho = \bar{s}_L \frac{1 - \rho^2}{1 - \rho^2 |s_L|^2},$$

$$R_\rho = r_\rho \circ \mathbf{c}^{-1}, \quad r_\rho = \rho \frac{1 - |s_L|^2}{1 - \rho^2 |s_L|^2}.$$

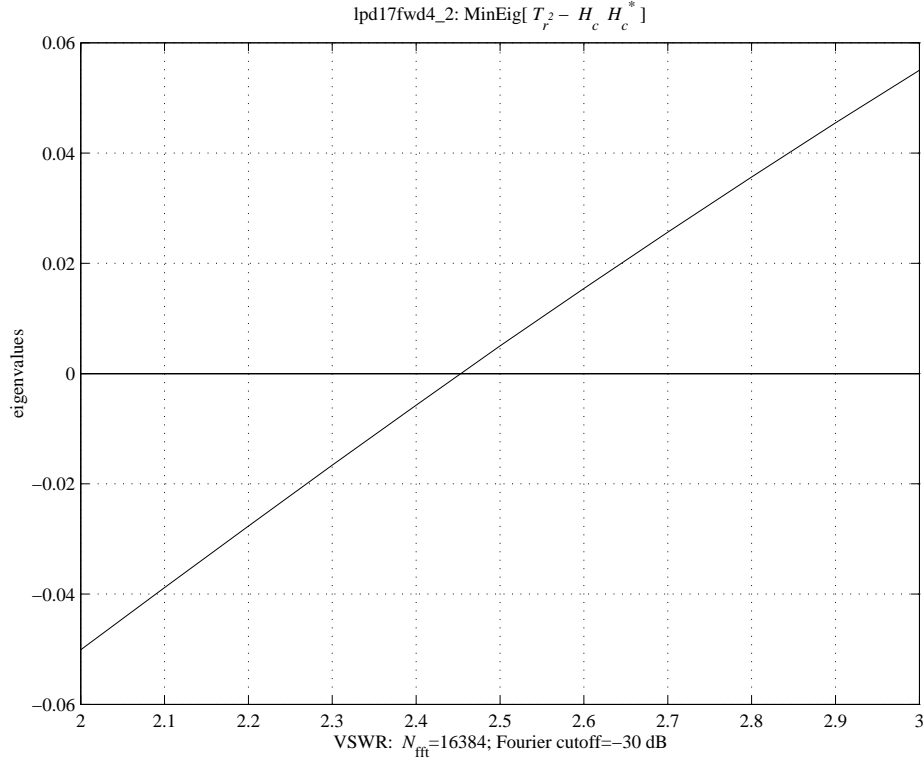


**Figure 24.** Estimate of  $\lambda_{\text{inf}}(\rho)$  versus  $\rho$  in terms of the VSWR

Let  $\lambda_{\text{inf}}(\rho)$  denote the smallest real number in the spectrum of  $\mathcal{T}_{R_\rho}^2 - \mathcal{H}_{C_\rho} \mathcal{H}_{C_\rho}^*$ . Figure 24 plots an estimate of  $\lambda_{\text{inf}}(\rho)$ . The optimal VSWR occurs near the zero-crossing point.

Figure 25 uses these VSWR bounds to benchmark several classes of matching circuits. Each circuit's VSWR is plotted as a function of the degree  $d$  (the total number of inductors and capacitors). The dashed lines are the VSWR from the low- and high-pass ladders containing inductors and capacitors constrained to practical design values. The solid line is the matching estimated from  $U^+(2, d)$ . A transformer performs as well as any matching circuit of degree 0 and as well as the low-pass ladders out to degree 6. The high-pass ladders get closer to the VSWR bound at degree 4. A perfectly coupled transformer (coefficient of coupling  $k = 1$ ) offers only a slight improvement over the transformer. In terms of making the tradeoff between VSWR and circuit complexity, Figure 25 directs the circuit designer's attention to the  $d = 2$  region. There exist matching circuits of order 2 with performance comparable to high-pass ladders of order 4. Thus, the circuit designer can graphically assess trade-offs between various circuits in the context of knowing the best match possible for any lossless 2-port.

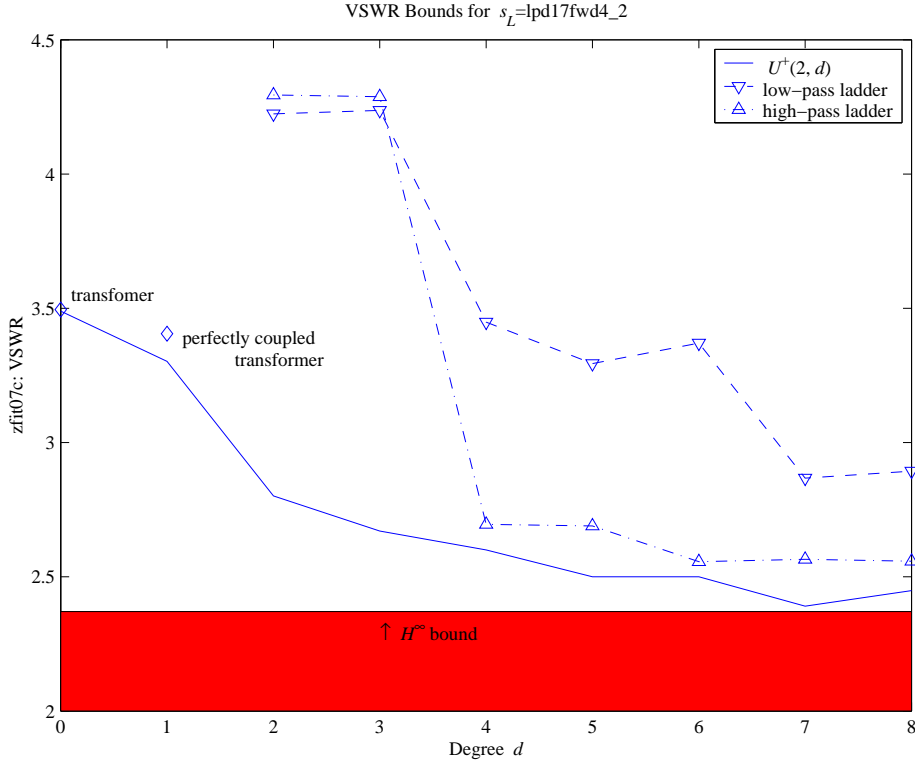


Figure 25. Comparing the matching performance of several classes of 2-ports with the Nehari and  $U^+(2, d)$  bounds.

### 9. Research Topics

This paper shows how to apply the Nehari bound to measured, real-world impedances. The price of admission is learning the scattering formalism and a few common electric circuits. The payoff is that many substantial research topics can be tastefully guided by this concrete problem. For immediate applications, several active and passive devices explicitly use wideband matching to improve performance:

- antenna [49; 2; 8; 1];
- circulator [36];
- fiber-optic links [7; 26; 23];
- satellite links [40];
- amplifiers [11; 22; 37].

The  $H^\infty$  applications to the transducers, antenna, and communication links are immediate. The amplifier is an active 2-port that requires a more general approach. The matching problem for the amplifier is to find input and output matching 2-ports that simultaneously maximize transducer power gain, minimize

the noise figure, and maintain stability. Although a more general problem, this amplifier-matching problem fits squarely in the  $H^\infty$  framework [28; 29; 30] and is a current topic in ONR’s  $H^\infty$  Research Initiative [41].

**9.1. Darlington’s Theorem and orbits.** Parameterizing the orbits currently limit the  $H^\infty$  approach and leads to a series of generalization on Darlington’s Theorem. An immediate application of Nehari’s Theorem asks for a “unit-ball” characterization of an orbit:

QUESTION 9.1. For what  $s_G \in BH^\infty(\mathbb{C}_+)$  is it true that  $\mathcal{F}_1(U^+(2, \infty), s_G)$  is dense in  $\text{Re } \bar{B}\mathcal{A}_1(\mathbb{C}_+)$ ?

This question of characterization is subsumed by the problem of computing orbits:

QUESTION 9.2. What is the orbit of a general reflectance  $\mathcal{F}_1(\mathcal{U}, s_L)$ ?

We can also generalize  $U^+(2, \infty)$  and ask about the orbit of  $s_L$  over all lumped 2-ports.

QUESTION 9.3. Characterize all reflectances that belong to

$$\overline{\bigcup_{d \geq 0} \mathcal{F}_1(U^+(2, d), s_L)}$$

Closely related is the question of *compatible impedances* or when a reflectance  $s_L$  belongs to the orbit of another reflectance  $s'_L$ .

QUESTION 9.4. Let  $s_L, s'_L \in \bar{B}H^\infty(\mathbb{C}_+)$ . Determine if there exists an  $S' \in U^+(2)$  such that  $s_L = \mathcal{F}_1(S', s'_L)$ .

The theory of compatible impedances is an active research topic in electrical engineering [54] and has links to the Buerling–Lax Theorem [29].

**9.2.  $U^+(2)$  and circuits.** The Circuit-Scattering Correspondence of Section 6 identified lumped, lossless  $N$ -ports and the scattering matrices of  $U^+(N, d)$  [52]. By identifying an  $N$ -port as a subset of a Hilbert space, Section 1 claimed that any linear, lossless, time-invariant, causal, maximal solvable  $N$ -port corresponded to a scattering matrix in  $U^+(N)$  [31]. The problem is reconcile the lumped approach, which has a concrete representation of a circuit, with Hilbert space claim, which gets a scattering matrix — not a circuit — by operator theory.

QUESTION 9.5. Does every element in  $U^+(2)$  correspond to a lossless 2-port?

In terms of Kirkoff’s current and voltage laws, if you were handed a collection of integro-differential partial differential equations, is it obvious that the system admits a scattering matrix?

**9.3. Circuit synthesis and matrix dilations.** If matching problem with  $s_G = 0$

$$\inf\{\|\Delta P(s_2, s_L)\|_\infty^2 : s_2 \in \mathcal{F}_2(U^+(2); 0)\},$$

admits a minimizer, then

$$s_2 = \mathcal{F}_2(S, s_G = 0) = s_{22} + s_{21}s_G(1 - s_{11}s_G)^{-1}s_{12}|_{s_G=0} = s_{22}.$$

How can we use  $s_2$  to get a matching scattering matrix  $S \in U^+(2)$ ? Thus, a circuit synthesis problem is really a question in matrix dilations.

QUESTION 9.6. Given  $s_2 \in \bar{B}H^\infty(\mathbb{C}_+)$ , find all  $S \in U^+(2)$  such that

$$S = \begin{bmatrix} s_{11} & s_{12} \\ s_{21} & s_{22} \end{bmatrix} = \begin{bmatrix} s_{11} & s_{12} \\ s_{21} & s_2 \end{bmatrix}.$$

Not all  $s_2$ 's can dilate to a lossless 2-port. Wohlers [52, page 100-101] shows that the 1-port with impedance  $z(p) = \arctan(p)$  cannot dilate to an  $S \in U^+(2)$ . The Douglas–Helton result characterizes those elements in the unit ball of  $H^\infty$  that came from a lossless  $N$ -port.

THEOREM 9.1 ([14; 15]). *Let  $S(p) \in \bar{B}H^\infty(\mathbb{C}_+, \mathbb{C}^{N \times N})$  be a real matrix function. The following are equivalent:*

- (A):  $S(p)$  admits an real inner dilation  $\mathbf{S}(p) = \begin{bmatrix} S(p) & S_{12}(p) \\ S_{21}(p) & S_{22}(p) \end{bmatrix}$ .
- (B):  $S(p)$  has a meromorphic pseudocontinuation of bounded type to the open left half-plane  $\mathbb{C}_-$ ; that is, there exist  $\phi \in H^\infty(\mathbb{C}_-)$  and  $H \in H^\infty(\mathbb{C}_-, \mathbb{C}^{N \times N})$  such that

$$\lim_{\substack{\sigma > 0 \\ \sigma \rightarrow 0}} S(\sigma + j\omega) = \lim_{\substack{\sigma > 0 \\ \sigma \rightarrow 0}} \frac{H}{\phi}(-\sigma + j\omega) \quad \text{a.e.}$$

- (C): There is an inner function  $\phi \in H^\infty(\mathbb{C}_+)$  such that  $\phi S^H \in H^\infty(\mathbb{C}_+, \mathbb{C}^{N \times N})$ .

Let  $\mathcal{M}$  denote the subset of  $\bar{B}H^\infty(\mathbb{C}_+)$  of functions that have meromorphic pseudocontinuations of bounded type. General hyperbolic Carleson–Jacob (Theorem 5.3) line of inquiry opens up to explore when the inequality

$$\inf\{\|\Delta P(s_2, s_L)\|_\infty : s_2 \in \mathcal{M}\} \geq \min\{\|\Delta P(s_2, s_L)\|_\infty^2 : s_2 \in \bar{B}H^\infty(\mathbb{C}_+)\}$$

holds with equality.

**9.4. Structure of  $U^+(2)$ .** Turning to the inclusion  $U^+(2, \infty) \subset U^+(2)$ , the preceding sections have established that  $U^+(2, \infty)$  is a closed subset of  $U^+(2)$  that consists of all rational inner functions parameterized by Belevitch's Theorem. Physically,  $U^+(2, \infty)$  models all the lumped 2-ports, but does not model the transmission line. It is natural to wonder what subclass of  $U^+(2)$  contains the lumped 2-ports and the transmission line. More precisely,

QUESTION 9.7. What constitutes a lumped-distributed network? How do we recognize its scattering matrix?

Wohlers [52] answers the first question by parameterizing the class of lumped-distributed  $N$ -ports, consisting of  $N_L$  inductors,  $N_C$  capacitors, and  $N_U$  uniform transmission lines using the model in Figure 26. Wohlers [52, pages 168–172]

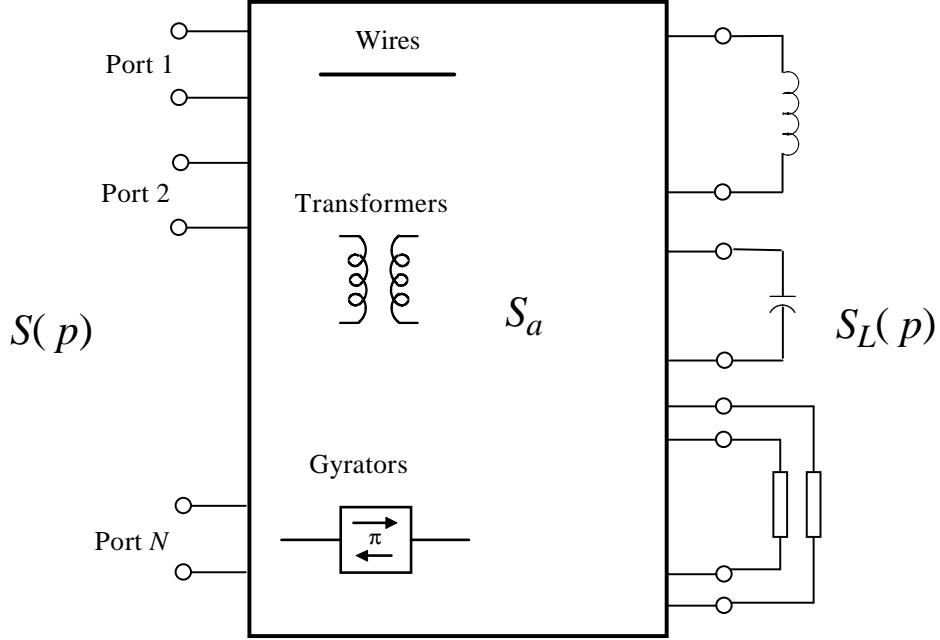


**Figure 26.** State-space representation of a lumped-distributed lossless 2-port.

establishes that such scattering matrices exist and have the form,

$$S(p) = \mathcal{F}(S_a, S_L; p) = S_{a,11} + S_{a,12}S_L(p)(I_d - S_{a,22}S_L(p))^{-1}S_{a,21},$$

where the augmented scattering matrix

$$S_a = \begin{bmatrix} S_{a,11} & S_{a,12} \\ S_{a,21} & S_{a,22} \end{bmatrix}$$

models a network of wires, transformers, and gyrators. Consequently,  $S_a$  is a constant, real, orthogonal matrix of size  $d = N_L + N_C + 2N_U$ .  $S_L(p)$  is called the augmented load and models the reactive elements as

$$S_L(p) = qI_{N_L} \oplus -qI_{N_C} \oplus \left\{ I_{N_U} \otimes \begin{bmatrix} 0 & e^{-\tau p} \\ e^{-\tau p} & 0 \end{bmatrix} \right\}.$$

This decomposition assumes: (1) the first  $N_L + N_C$  ports are normalized to  $z_0 = 1$ , and (2) the remaining  $N_U$  pairs of ports are normalized to the characteristic impedance  $Z_{0,n_u}$  of each transmission line. Although some work has been done characterizing these scattering matrices, the reports in Wohlers [52, page 173] are false, as determined by Choi [10].

**9.5. Error bounds.** The problem is to determine if  $\mathcal{T}_{r^2} \geq \mathcal{H}_c^* \mathcal{H}_c$ , when all we know are noisy samples of the center and radius functions measured at a finite number of frequencies. Of the several approaches to this problem [29], we use the simple Spline-FFT Method.

THE SPLINE-FFT NEHARI ALGORITHM *Given samples  $\{(j\omega_k, C(j\omega_k))\}$  and  $\{(j\omega_k, R(j\omega_k))\}$ , where  $0 \leq \omega_1 < \omega_2 < \dots < \omega_K < \infty$ .*

SF-1: *Cayley transform the samples from  $j\mathbb{R}$  to the unit circle  $\mathbf{T}$ :*

$$c(e^{j\theta_k}) := C \circ \mathbf{c}^{-1}(e^{j\theta_k}), \quad r(e^{j\theta_k}) := R \circ \mathbf{c}^{-1}(e^{j\theta_k}).$$

SF-2: *Use a spline to extend  $\{e^{j\theta_k}, c(e^{j\theta_k})\}$  and  $\{e^{j\theta_k}, r(e^{j\theta_k})\}$  to functions on the unit circle  $\mathbf{T}$ .*

SF-3: *Approximate the Fourier coefficients using the FFT:*

$$\begin{aligned} \widehat{c}(N; n) &:= \frac{1}{N} \sum_{n'=0}^{N-1} e^{-j2\pi n n' / N} c(e^{+j2\pi n' / N}), \\ \widehat{r}(N; n) &:= \frac{1}{N} \sum_{n'=0}^{N-1} e^{-j2\pi n n' / N} r(e^{+j2\pi n' / N}). \end{aligned}$$

SF-4: *Make the truncated Toeplitz and Hankel matrices:*

$$\begin{aligned} \mathcal{T}_{r^2, M, N} &= \left[ \widehat{r}^2(N; m_1 - m_2) \right]_{m_1, m_2=0}^{M-1}, \\ \mathcal{H}_{c, M, N} &= \left[ \widehat{c}(N; -(m_1 + m_2)) \right]_{m_1, m_2=0}^{M-1}. \end{aligned}$$

SF-5: *Find the smallest eigenvalue of*

$$A_{M, N} := \mathcal{T}_{r^2, M, N} - \mathcal{H}_{c, M, N}^H \mathcal{H}_{c, M, N}.$$

We are aware of the following sources of error:

- The samples are corrupted by measurement errors.
- The spline extensions from sampled data to functions defined on the unit circle  $\mathbf{T}$ .
- The Fourier coefficients are computed from an FFT of size  $N$ .
- The operator  $A$  is computed from  $M \times M$  truncations.

QUESTION 9.8. Are these all the sources of error (neglecting roundoff)? How can the Spline-FFT Nehari algorithm adapt to account for these errors? Can we put error bars on Figure 24?

## 10. Epilogue

One of the great joys in applied mathematics is to link an abstract computation to a physical system. Nehari's Theorem computes the norm of a Hankel operator  $\mathcal{H}_\phi$  as the distance between its symbol  $\phi \in L^\infty$  and the Hardy subspace  $H^\infty$ :

$$\|\mathcal{H}_\phi\| = \inf\{\|\phi - h\|_\infty : h \in H^\infty\}.$$

One of J. W. Helton's inspired observations linked this computation to a host of problems in electrical engineering and control theory. These problems, in turn, led Helton to deep and original extensions of operator theory, geometry, convex analysis, and optimization theory.

By linking  $H^\infty$  theory to the matching circuits, a physical meaning is attached to the Nehari computation and produces a plot that the electrical engineers can actually use. Along the way we encountered Darlington's Theorem, Belevitch's Theorem, Weierstrass' Theorem, the Carleson–Jacobs theorems, Nehari's Theorem, inner-function models, and hyperbolic geometry. Impedance-matching provides a case study of rather surprising mathematical richness in what may appear at first to be a rather prosaic analog signal processing issue.

A measure of the vitality of a subject is the quality of the unexplored questions. A small effort invested in circuit theory opens up a host of wonderful research topics for mathematicians. These topics discussed in this paper indicate only a few of the significant research opportunities that lie between mathematics and electrical engineering. For the mathematician, there are few engineering subjects where an advanced topic like  $H^\infty$  has such an immediate connection actual physical devices. We hope our readers do realize a rich harvest from these research opportunities.

### Appendix A. Matrix-Valued Factorizations

This appendix proves Corollary 6.1 using Blaschke–Potapov factorizations. We start with the scalar-valued case.

LEMMA A.1. *Let  $h \in H^\infty(\mathbf{D})$  be an inner function. The following are equivalent:*

- (A):  $h \in \mathcal{A}(\mathbf{D})$ .
- (B):  $h$  is rational.

PROOF. (a  $\implies$  b) Factor  $h$  as  $h = cbs$ , where  $c \in \mathbf{T}$ ,  $b$  is a Blaschke and  $s$  is a singular inner function. If  $z_a \in \mathbf{T}$  is an accumulation point of the zeros  $\{z_n\}$  of  $b$ , that is, there is a subsequence  $z_{n_k} \rightarrow z_a$ , then continuity of  $h$  on  $\overline{\mathbf{D}}$  implies that  $0 = h(z_{n_k}) \rightarrow h(z_a)$ . Continuity of  $h$  on  $\overline{\mathbf{D}}$  gives a neighborhood  $U \subset \mathbf{T}$  of  $z_a$  for which  $|h(U)| < 1$ . Thus,  $h$  cannot be inner with  $b$  an infinite Blaschke product. Thus,  $b$  can only be a finite product and has no accumulation points to cancel the discontinuities of  $s$ . More formally,  $b$  never vanishes on  $\mathbf{T}$  and neither

$s$  nor  $|s|$  is continuously extendable to from the interior of the disk to any point in the support of the singular measure that represents  $s$  [35, pages 68–69]. Thus,  $h$  cannot have a singular part and we have  $h = cb$ .

(b  $\implies$  a) A rational  $h$  also in  $H^\infty(\mathbf{D})$  cannot have a pole in  $\overline{\mathbf{D}}$ . Then  $h$  is continuous on  $\overline{\mathbf{D}}$  so belongs to the disk algebra.  $\square$

The result generalizes to matrix-valued inner functions. For  $a \in \mathbf{D}$ , define the elementary Blaschke factor [38, Equation 4.2]:

$$b_a(z) := \begin{cases} \frac{|a|}{a} \frac{a-z}{1-\bar{a}z} & \text{if } a \neq 0, \\ z & \text{if } a = 0. \end{cases}$$

To get a matrix-valued version, let  $P \in \mathbb{C}^{N \times N}$  be an orthogonal projection:  $P^2 = P$  and  $P^H = P$ . The *Blaschke–Potapov elementary factor* associated with  $a$  and  $P$  is [38, Equation 4.4]:

$$B_{a,P}(z) := I_M + (b_a(z) - 1)P.$$

There are a couple of ways to see that  $B_{a,P}$  is inner. Let  $U$  be a unitary matrix that diagonalizes  $P$ :

$$U^H P U = \begin{bmatrix} I_K & 0 \\ 0 & 0 \end{bmatrix}.$$

Then,

$$U^H B_{a,P}(z) U = \begin{bmatrix} b_a(z) I_K & 0 \\ 0 & I_{M-K} \end{bmatrix}.$$

From this, we get [38, Equation 4.5]:

$$\det[B_{a,P}(z)] = b_a(z)^{\text{rank}[P]}.$$

DEFINITION A.1 ([38, pages 320–321]). The function  $B : \mathbf{D} \rightarrow \mathbb{C}^{N \times N}$  is called a *left Blaschke–Potapov product* if either  $B$  is a constant unitary matrix or there exists a unitary matrix  $U$ , a sequence of orthogonal projection matrices  $\{P_k : k \in \mathcal{K}\}$ , and a sequence  $\{z_k : k \in \mathcal{K}\} \subset \mathbf{D}$  such that

$$\sum_{k \in \mathcal{K}} (1 - |z_k|) \text{trace}[P_k] < \infty$$

and the representation

$$B(z) = \left\{ \prod_{k \in \mathcal{K}}^{\rightarrow} B_{z_k, P_k}(z) \right\} U$$

holds.

DEFINITION A.2 ([38, pages 319]). Let  $S \in H^\infty(\mathbf{D}, \mathbb{C}^{N \times N})$  be an inner function.  $S$  is called *singular* if and only if  $\det[S(z)] \neq 0$  for all  $z \in \mathbf{D}$ .

THEOREM A.1 ([38, Theorem 4.1]). *Let  $S \in H^\infty(\mathbf{D}, \mathbb{C}^{N \times N})$  be an inner function. There exists a left Blaschke–Potapov product and a  $\mathbb{C}^{N \times N}$ -valued singular inner function  $\Xi$  such that*

$$S = B\Xi.$$

Moreover, the representation is unique up to a unitary matrix  $U$ . If

$$S = B_1\Xi_1 = B_2\Xi_2,$$

then  $B_2 = B_1U$  and  $\Xi_2 = U^H\Xi_1$ .

Critical for our use is that the determinant maps these matrix-valued generalizations of the Blaschke and singular functions to their scalar-valued counterparts.

THEOREM A.2 ([38, Theorem 4.2]). *Let  $S \in \bar{B}H^\infty(\mathbf{D}, \mathbb{C}^{N \times N})$ .*

(A):  $\det[S] \in \bar{B}H^\infty(\mathbf{D})$ .

(B):  $S$  is inner if and only if  $\det[S]$  is inner.

(C):  $S$  is singular if and only if  $\det[S]$  is singular.

With these results in place, Lemma A.1 generalizes to the matrix-valued case.

PROOF OF COROLLARY A.1. (a  $\implies$  b) Lemma 3.3 and Assumption (a) give that  $W = S \circ \mathbf{c}^{-1}$  is a continuous inner function in  $\mathcal{A}(\mathbf{D}, \mathbb{C}^{2 \times 2})$ . Theorem A.1 gives that  $W = B\Xi$  for a left Blaschke–Potapov product  $B$  and singular  $\Xi$ . Observe that  $\det[W] = \det[B]\det[\Xi]$ . If  $W$  is inner, then  $\det[W]$  is inner by Theorem A.2(a). Because  $W$  is continuous,  $\det[W]$  is continuous and Lemma A.1 forces  $\det[W]$  to be rational. Therefore,  $\det[W]$  cannot admit the singular factor  $\det[\Xi]$ . Consequently,  $W$  cannot have a singular factor by Theorem A.2(c). Because  $\det[W]$  is rational and

$$\det[W] = \det[B] = \prod b_{z_k}^{\text{rank}[P_k]},$$

we see that  $B$  must be a *finite* left Blaschke–Potapov product. Consequently,  $S = W \circ \mathbf{c}$  is rational. Finally, this gives that  $S$  is rational.

(b  $\implies$  a) Let

$$S(p) = \frac{1}{g(p)}H(p),$$

where  $g(p)$  is a real polynomial

$$g(p) = g_0 + g_1p + \cdots + g_Lp^L,$$

of degree  $K$  that is strict Hurwitz (zero only in  $\mathbb{C}_-$ ) and  $H(p)$  is a real  $N \times N$  polynomial

$$H(p) = H_0 + H_1p + \cdots + H_Mp^M$$

of degree  $L$ . Boundedness forces  $L \geq M$ . Then,

$$\frac{H(p)}{g(p)} = \frac{H_0 + \cdots + H_Mp^M}{g_0 + \cdots + g_Lp^L} \xrightarrow{p \rightarrow \infty} \begin{cases} 0 & \text{if } L > M, \\ H_N/g_N & \text{if } L = M. \end{cases}$$

Thus,  $H(p)/g(p)$  is continuous across  $p = \pm j\infty$ . Thus,  $S(p)$  is continuous at  $\pm j\infty$ .  $\square$

### Appendix B. Proof of Lemma 4.4

The chain scattering representations are [25]:

$$\mathfrak{G}(\Theta_1; s) := \mathcal{F}_1(S, s), \quad \Theta_1 \sim \frac{1}{s_{21}} \begin{bmatrix} -\det[S] & s_{11} \\ -s_{22} & 1 \end{bmatrix},$$

$$\mathfrak{G}(\Theta_2; s) := \mathcal{F}_2(S, s), \quad \Theta_2 \sim \frac{1}{s_{12}} \begin{bmatrix} -\det[S] & s_{22} \\ -s_{11} & 1 \end{bmatrix},$$

where “ $\sim$ ” denotes equality in homogeneous coordinates:  $\Theta \sim \Phi$  if and only if  $\mathfrak{G}(\Theta) = \mathfrak{G}(\Phi)$ . Because  $S(p)$  is unitary on  $j\mathbb{R}$ ,  $\Theta_1(p)$  and  $\Theta_2(p)$  are  $J$ -unitary on  $j\mathbb{R}$  [29]:

$$\Theta^H J \Theta = J = \begin{bmatrix} 1 & 0 \\ 0 & -1 \end{bmatrix}.$$

Fix  $\omega \in \mathbb{R}$ . Define the maps  $\mathbf{g}_1$  and  $\mathbf{g}_2$  on the unit disk  $\mathbf{D}$  as

$$\mathbf{g}_1(s) := \mathfrak{G}(\Theta_1(j\omega), s), \quad \mathbf{g}_2(s) := \mathfrak{G}(\Theta_2(j\omega), s).$$

Because  $\Theta_1(p)$  and  $\Theta_2(p)$  are  $J$ -unitary on  $j\mathbb{R}$ , it follows that  $\mathbf{g}_1$  and  $\mathbf{g}_2$  are invertible automorphisms of the unit disk onto itself with inverses:

$$\mathbf{g}_1^{-1}(s) = \mathfrak{G}(\Theta_1(j\omega)^{-1}, s), \quad \Theta_1(j\omega)^{-1} \sim \begin{bmatrix} -1 & s_{11}(j\omega) \\ -s_{22}(j\omega) & \det[S(j\omega)] \end{bmatrix}$$

$$\mathbf{g}_2^{-1}(s) = \mathfrak{G}(\Theta_2(j\omega)^{-1}, s), \quad \Theta_2(j\omega)^{-1} \sim \begin{bmatrix} -1 & s_{22}(j\omega) \\ -s_{11}(j\omega) & \det[S(j\omega)] \end{bmatrix}.$$

Because the  $\mathbf{g}_k$ 's and their inverses are invertible automorphisms, Equation 4–9 gives that

$$\left| \frac{\mathbf{g}(s_1) - \mathbf{g}(s_2)}{1 - \mathbf{g}(s_1)\overline{\mathbf{g}(s_2)}} \right| = \left| \frac{s_1 - s_2}{1 - s_1\overline{s_2}} \right|,$$

for  $s_1, s_2 \in \mathbf{D}$  and  $\mathbf{g}$  denoting either  $\mathbf{g}_1, \mathbf{g}_2, \mathbf{g}_1^{-1}$ , or  $\mathbf{g}_2^{-1}$ . For all  $p \in j\mathbb{R}$ , we obtain

$$\begin{aligned} \Delta P(s_2, s_L) &= \left| \frac{s_2 - \overline{s_L}}{1 - s_2 s_L} \right| = \left| \frac{\mathbf{g}_2(s_G) - \overline{s_L}}{1 - \mathbf{g}_2(s_G) s_L} \right| \\ &= \left| \frac{s_G - \mathbf{g}_2^{-1}(\overline{s_L})}{1 - s_G \mathbf{g}_2^{-1}(\overline{s_L})} \right| = \Delta P(s_G, \overline{\mathbf{g}_2^{-1}(\overline{s_L})}). \end{aligned}$$

Then  $\Delta P(s_2, s_L) = \Delta P(s_G, s_1)$ , provided we can show  $s_1 = \overline{\mathbf{g}_2^{-1}(\overline{s_L})}$ . In terms of the chain matrices, this requires us to show

$$s_1 = \mathfrak{G}(\Theta_1; s_L) = \overline{\mathfrak{G}(\Theta_2^{-1}; \overline{s_L})} = \mathfrak{G}(\Theta_2^{-1}; s_L).$$

This equality will follow if we can show  $\Theta_1 \sim \overline{\Theta_2^{-1}}$  or that

$$\Theta_1 \sim \begin{bmatrix} -1 & s_{11}/\det[S] \\ -s_{22}/\det[S] & 1/\det[S] \end{bmatrix} \sim \begin{bmatrix} -1 & \overline{s_{22}} \\ -\overline{s_{11}} & \overline{\det[S]} \end{bmatrix} \sim \overline{\Theta_2^{-1}}.$$

Because  $S(p)$  is inner,  $\det[S]$  is inner so that  $\overline{\det[S]} = 1/\det[S]$  on  $j\mathbb{R}$ . Also, on  $j\mathbb{R}$ ,  $S(p)$  is unitary so that

$$S^{-1} = \frac{1}{\det[S]} \begin{bmatrix} s_{22} & -s_{12} \\ -s_{21} & s_{11} \end{bmatrix} = \begin{bmatrix} \overline{s_{11}} & \overline{s_{12}} \\ \overline{s_{21}} & \overline{s_{22}} \end{bmatrix}.$$

Then,  $\overline{s_{22}} = s_{11}/\det[S]$  and  $\overline{s_{11}} = s_{22}/\det[S]$ . Thus,  $\Theta_1 \sim \overline{\Theta_2^{-1}}$  so that  $s_1 = \overline{g_2^{-1}(\overline{s_L})}$  or that the LFT law holds. By Lemma 4.3, the LFT laws give the TGP laws.

### Appendix C. Proof of Theorem 6.1

Let  $C(\mathbf{T}, \mathbb{C}^{N \times N})$  denote the continuous functions on the unit circle  $\mathbf{T}$ . Let  $\mathcal{R}_M^L$  denote those rational functions  $g^{-1}(q)H(q)$  in  $C(\mathbf{T}, \mathbb{C}^{N \times N})$  where  $g(q)$  and  $H(q)$  are polynomials with degrees  $\partial[g] \leq M$  and  $\partial[H] \leq L$ . The Existence Theorem [9, page 154] shows that  $\mathcal{R}_M^L$  is a boundedly compact subset of  $C(\mathbf{T}, \mathbb{C}^{N \times N})$ . Lemma 3.3 shows the Cayley transform preserves compactness. Thus,  $\mathcal{R}_M^L \circ \mathbf{c}$  is a boundedly compact subset of  $1 \dot{+} C(j\mathbb{R}, \mathbb{C}^{N \times N})$ . By Lemma 3.1,  $U^+(N)$  is a closed subset of  $L^\infty(j\mathbb{R}, \mathbb{C}^{N \times N})$ . The intersection of a closed and bounded set with a boundedly compact set is compact. Thus,  $U^+(N) \cap \mathcal{R}_M^L \circ \mathbf{c}$  is a compact subset of  $1 \dot{+} C(j\mathbb{R}, \mathbb{C}^{N \times N})$ . We claim that  $U^+(N, d) = U^+(N) \cap \mathcal{R}_d^d \circ \mathbf{c}$ . Observe  $\mathcal{R}_d^d \circ \mathbf{c}$  consists of all rational functions with the degree of the numerator and denominator not exceeding  $d$  and that are also continuous on  $j\mathbb{R}$ , including the point at infinity. If  $S \in U^+(N) \cap \mathcal{R}_d^d \circ \mathbf{c}$ , then  $\deg_{\text{SM}}[S] \leq d$ . This forces  $S$  into  $U^+(N, d)$ . Consequently,  $U^+(N, d) \supseteq U^+(N) \cap \mathcal{R}_d^d \circ \mathbf{c}$ . For the converse, suppose  $S \in U^+(N, d)$ . By Corollary 6.1,  $S \in \mathcal{A}_1(\mathbb{C}_+, \mathbb{C}^{N \times N})$  and thus forces  $S$  into  $\mathcal{R}_d^d \circ \mathbf{c}$ . Thus,  $U^+(N, d) \subseteq U^+(N) \cap \mathcal{R}_d^d \circ \mathbf{c}$  and equality must hold. Thus,  $U^+(N, d)$  is compact.

### Appendix D. Proof of Theorem 5.5

We start by remarking upon the disk with strict inequalities:

$$D(c, r) := \{\phi \in L^\infty(j\mathbb{R}) : |\phi(j\omega) - c(j\omega)| < r(j\omega) \quad \text{a.e.}\}.$$

First,  $D(c, r)$  need not be open. For example,  $D(0, 1)$  contains the open unit ball and is contained in its closure:

$$BL^\infty(j\mathbb{R}) \subset D(0, 1) \subset \overline{BL^\infty(j\mathbb{R})}.$$

However,

$$\phi(j\omega) := \frac{\omega}{1 + |\omega|}$$

belongs to  $D(0,1)$  but with  $\|\phi\|_\infty = 1$ , there is no neighborhood of  $\phi$  that is contained in the open unit ball.

Second, consider what the strict inequalities mean for those  $\gamma : L^\infty(j\mathbb{R}) \rightarrow \mathbb{R}$  that are continuous with sublevel sets

$$[\gamma \leq \alpha] = \bar{D}(c_\alpha, r_\alpha).$$

We cannot claim that  $[\gamma < \alpha]$  is  $D(c_\alpha, r_\alpha)$ . Instead,  $[\gamma < \alpha]$  is an *open set* contained by  $D(c_\alpha, r_\alpha)$ . In this regard, the following result gives us some control of the strict inequality.

**THEOREM D.1.** *Let  $c, r \in L^\infty(j\mathbb{R})$ . Assume  $r^{-1} \in L^\infty(j\mathbb{R})$ . Let  $V$  be any nonempty open subset of  $L^\infty(j\mathbb{R})$  such that  $V \subseteq D(c, r)$ . For any  $\phi \in V$ ,*

$$\|r^{-1}(\phi - c)\|_\infty < 1.$$

**PROOF.** For any  $\phi \in V$ , the openness of  $V$  implies there is an  $\varepsilon > 0$  such that

$$\phi + \varepsilon BL^\infty(j\mathbb{R}) \subset V.$$

Consider the particular element of the open ball:

$$\Delta\phi := \varepsilon' \times \operatorname{sgn}(\phi - c) \frac{r}{\|r\|_\infty},$$

where  $0 < \varepsilon' < \varepsilon$  and

$$\operatorname{sgn}(z) := \begin{cases} z/|z| & \text{if } z \neq 0, \\ 0 & \text{if } z = 0. \end{cases}$$

Then  $\phi + \Delta\phi \in D(c, r)$  so that

$$r > |\phi + \Delta\phi - c| = |\phi - c| + \varepsilon' \frac{r}{\|r\|_\infty} \quad \text{a.e.}$$

Divide by  $r$  and take the norm to get

$$1 \geq \|r^{-1}(\phi - c)\|_\infty + \varepsilon' \|r\|_\infty^{-1},$$

or that  $1 > \|r^{-1}(\phi - c)\|_\infty$ . To complete the argument, we need to demonstrate that the preceding argument is not vacuous. That is,  $D(c, r)$  does indeed contain an open set. Because  $r$  does not “pinch off”,  $0 < \|r\|_{-\infty}$ . Choose any  $0 < \eta < \|r\|_{-\infty}$ . For any  $\phi \in BL^\infty(j\mathbb{R})$

$$\|(\eta\phi + c) - c\|_\infty \leq \eta < r \quad \text{a.e.}$$

Thus, the open set  $c + \eta BL^\infty(j\mathbb{R})$  is contained in  $D(c, r)$ .  $\square$

PROOF OF THEOREM 5.5. There always holds

$$\begin{aligned} \rho_{\bar{B}A_1} &:= \inf\{\|\Delta P(s_2, s_L)\|_\infty : s_2 \in \bar{B}A_1(\mathbb{C}_+)\} \\ &\geq \min\{\|\Delta P(s_2, s_L)\|_\infty : s_2 \in \bar{B}H^\infty(\mathbb{C}_+)\} = \rho_{\bar{B}H^\infty}. \end{aligned}$$

Suppose the inequality is strict. Then there is an  $s_2 \in \bar{B}H^\infty(\mathbb{C}_+)$  such that

$$\rho_{\bar{B}A_1} > \|\Delta P(s_2, s_L)\|_\infty. \quad (\text{D-1})$$

By Lemma 4.6, the mapping  $\Delta\rho(s_2) := \|\Delta P(s_2, s_L)\|_\infty$  is a continuous function on  $\bar{B}L^\infty(j\mathbb{R})$ . Consequently,  $[\Delta\rho < \rho_{\bar{B}A_1}]$  is open with

$$[\Delta\rho < \rho_{\bar{B}A_1}] \subset D(k_A, r_A),$$

where the center function and radius functions are

$$k_A := \bar{s}_L \frac{1 - \rho_{\bar{B}A_1}^2}{1 - \rho_{\bar{B}A_1}^2 |s_L|^2}, \quad r_A := \rho_{\bar{B}A_1} \frac{1 - |s_L|^2}{1 - \rho_{\bar{B}A_1}^2 |s_L|^2}.$$

Let  $r_A$  have spectral factorization  $r_A = |q_A|$ . By Theorem D.1,

$$\|q_A^{-1}k_A - q_A^{-1}s_2\|_\infty < 1.$$

If we assume that  $q_A^{-1}k_A \in 1\dot{+}C_0(j\mathbb{R})$ , Theorem 5.2 forces equality:

$$1 > \|q_A^{-1}k_A - H^\infty(\mathbb{C}_+)\|_\infty = \|q_A^{-1}k_A - \mathcal{A}_1(\mathbb{C}_+)\|_\infty.$$

The equality lets us select  $s_A \in \mathcal{A}_1(\mathbb{C}_+)$  that satisfies

$$1 - \varepsilon_0 > \|q_A^{-1}(k_A - s_A)\|_\infty,$$

for some  $1 > \varepsilon_0 > 0$ . This forces the pointwise result:

$$(1 - \varepsilon_0)r_A \geq |k_A - s_A| \quad \text{a.e.}$$

With some effort, we will show that this pointwise equality implies

$$\Delta\rho(s_A) < \rho_{\bar{B}A_1}.$$

This contradiction implies that Equation D-1 cannot be true or that the inequality  $\rho_{\bar{B}A_1} \geq \rho_{\bar{B}H^\infty}$  cannot be strict.

To start this demonstration, we first prove  $q_A^{-1}k_A$  is continuous. Because  $s_L$  belongs to the open unit ball of the disk algebra, both  $k_A$  and  $r_A$  belong to  $1\dot{+}C_0(j\mathbb{R})$ . Thus, it remains to prove that  $q_A^{-1}$  is continuous. Lemma 3.3 gives that  $R_A = r_A \circ \mathbf{c}^{-1}$  belongs to  $C(\mathbf{T})$ . Ignore the trivial case when  $\rho_{\bar{B}A_1} = 0$ . Because

$$R_A \geq \rho_{\bar{B}A_1}(1 - \|s_L\|_\infty^2) > 0$$

it follows that  $\log(R_A) \in C(\mathbf{T})$  and defines the outer function [18, page 24]:

$$Q_A(z) := \exp\left(\frac{1}{2\pi} \int_0^{2\pi} \frac{e^{jt} + z}{e^{jt} - z} \log(R_A(e^{jt})) dt\right) \in \mathcal{A}(\mathbf{D}).$$

Lemma 3.3 gives that  $q_{\mathcal{A}} = Q_{\mathcal{A}} \circ \mathbf{c} \in \mathcal{A}_1(\mathbb{C}_+)$  and is also an outer function. Because  $q_{\mathcal{A}}$  is an outer function  $q_{\mathcal{A}}^{-1} \in \mathcal{A}_1(\mathbb{C}_+)$ . Thus, a spectral factorization exists in the disk algebra.

To continue, define for  $\varepsilon \in [0, \varepsilon_0]$ ,

$$\rho(\varepsilon) := (1 - \varepsilon)\rho_{\bar{B}_{A_1}}.$$

Define

$$k_\varepsilon := \bar{s}_L \frac{1 - \rho(\varepsilon)^2}{1 - \rho(\varepsilon)^2 |s_L|^2}, \quad r_\varepsilon := \rho_\rho(\varepsilon) \frac{1 - |s_L|^2}{1 - \rho(\varepsilon)^2 |s_L|^2}.$$

In  $L^\infty(j\mathbb{R})$ ,  $k_\varepsilon \rightarrow k_{\mathcal{A}}$  and  $r_\varepsilon \rightarrow r_{\mathcal{A}}$  as  $\varepsilon \rightarrow 0$ . Then

$$\begin{aligned} |s_{\mathcal{A}} - k_\varepsilon| &\leq |s_{\mathcal{A}} - k_{\mathcal{A}}| + |k_{\mathcal{A}} - k_\varepsilon| \\ &\leq (1 - \varepsilon_0)r_{\mathcal{A}} + |k_{\mathcal{A}} - k_\varepsilon| \leq (1 - \varepsilon_0)r_\varepsilon + |r_{\mathcal{A}} - r_\varepsilon| + |k_{\mathcal{A}} - k_\varepsilon|. \end{aligned}$$

Because the last two terms are bounded as  $\mathcal{O}[\varepsilon]$ ,

$$|s_{\mathcal{A}} - k_\varepsilon| \leq r_\varepsilon - \varepsilon_0 r_\varepsilon + \mathcal{O}[\varepsilon].$$

Because  $r_{\mathcal{A}}$  is uniformly positive, and  $r_\varepsilon$  converges to  $r_{\mathcal{A}}$ , the last two terms are uniformly negative for all  $\varepsilon > 0$  sufficiently small. This puts

$$s_{\mathcal{A}} \in \bar{D}(k_\varepsilon, r_\varepsilon) \iff \Delta\rho(s_{\mathcal{A}}) < (1 - \varepsilon)\rho_{\bar{B}_{A_1}}. \quad \square$$

## References

- [1] J. C. Allen and David F. Schwartz, *User's guide to antenna impedance models and datasets*, SPAWAR TN **1791**, 1998.
- [2] Hongming An, B. K. J. C. Nauwelaers, and A. R. Van de Capelle, "Broadband microstrip antenna design with the simplified real frequency technique", *IEEE Transactions on Antennas and Propagation* **42:2** (1994).
- [3] H. Baher, *Synthesis of electrical networks*, Wiley, New York, 1984.
- [4] Norman Balabanian and Theodore A. Bickart, *Linear network theory*, Matrix Publishers, Beaverton (OR), 1981.
- [5] Lennart Carleson and Sigvard Jacobs, "Best uniform approximation by analytic functions", *Arkiv för Matematik* **10** (1972), 219–229.
- [6] Joseph J. Carr, *Practical antenna handbook*, Tab Books, Blue Ridge Summit (PA), 1989.
- [7] Michael de la Chapelle, "Computer-aided analysis and design of microwave fiber-optic links", *Microwave Journal* **32:9** (1989).
- [8] Nan-Cheng Chen, H. C. Su, and K. L. Wong "Analysis of a broadband slot-coupled dielectric-coated hemispherical dielectric resonator antenna", *Microwave and Optical Technology Letters* **8:1** (1995).
- [9] E. W. Cheney, *Approximation theory*, Chelsea, New York, 1982.
- [10] Man-Duen Choi, "Positive semidefinite biquadratic forms", *Linear Alg. Appl.* **12** (1975), 95–100.

- [11] Kenneth R. Cioffi, “Broad-band distributed amplifier impedance-matching techniques”, *IEEE Transactions on Microwave Theory and Techniques* **37**:12 (1989).
- [12] Eva Decker, “On the boundary behavior of singular inner functions”, *Michigan Math. J.* **41**:3 (1994), 547–562.
- [13] R. G. Douglas, *Banach algebra techniques in operator theory*, Academic Press, New York, 1972.
- [14] R. G. Douglas and J. W. Helton, “The precise theoretical limits of causal Darlington synthesis”, *IEEE Transactions on Circuit Theory*, CT-20, Number 3 (1973), 327.
- [15] R. G. Douglas and J. W. Helton, “Inner dilations of analytic matrix functions and Darlington synthesis”, *Acta Sci. Math. (Szeged)*, **43** (1973), 61–67.
- [16] Janusz A. Dobrowolski and Wojciech Ostrowski *Computer-aided analysis, modeling, and design of microwave networks*, Artech House, Boston (MA), 1996.
- [17] Nelson Dunford and Jacob T. Schwartz, *Linear Operators*, Part I, Interscience, New York, 1967.
- [18] Peter L. Duren, *Theory of  $H^p$  spaces*, Academic Press, New York, 1970.
- [19] J. B. Garnett, *Bounded analytic functions*, Academic Press, New York, 1981.
- [20] Kazimierz Geobel and Simeon Reich *Uniform convexity, hyperbolic geometry, and nonexpansive mappings*, Marcel Dekker, New York, 1984.
- [21] Guillermo Gonzalez, *Microwave transistor amplifiers*, 2nd edition, Prentice Hall, Upper Saddle River (NJ), 1997.
- [22] Anthony N. Gerkis, “Broadband impedance matching using the real frequency network synthesis technique”, *Applied Microwave and Wireless* (1998).
- [23] A. Ghiasi and A. Gopinath, “Novel wide-bandwidth matching technique for laser diodes”, *IEEE Transactions on Microwave Theory and Techniques* **38**:5 (1990), 673–675.
- [24] Charles L. Goldsmith and Brad Kanack, Broad-band reactive matching of high-speed directly modulated laser diodes, *IEEE Microwave and Guided Wave Letters* **3**:9 (1993), 336–338.
- [25] Martin Hasler and Jacques Neiryneck, *Electric filters*, Artech House, Dedham (MA), 1986.
- [26] Roger Helkey, J. C. Twichell, and Charles Cox, “A down-conversion optical link with RF gain”, *J. Lightwave Technology* **15**:5 (1997).
- [27] Henry Helson, *Harmonic analysis*, Addison-Wesley, Reading (MA), 1983.
- [28] J. William Helton, “Broadbanding: gain equalization directly from data”, *IEEE Transactions on Circuits and Systems*, CAS-28, Number 12 (1981), 1125–1137.
- [29] J. William Helton, “Non-Euclidean functional analysis and electronics”, *Bull. Amer. Math. Soc.* **7**:1 (1982), 1–64.
- [30] J. William Helton, “A systematic theory of worst-case optimization in the frequency domain: high-frequency amplifiers”, *IEEE ISCAS*, Newport Beach (CA), 1983.

- [31] J. William Helton, [1987] *Operator theory, analytic functions, matrices, and electrical engineering*, CBMS Regional Conference Series **68**, Amer. Math. Soc., Providence, 1987.
- [32] J. William Helton and Orlando Merino, *Classical control using  $H^\infty$  methods*, SIAM, Philadelphia, 1998.
- [33] William Hintzman, “Best uniform approximations via annihilating measures”, *Bull. Amer. Math. Soc.* **76** (1975), 1062–1066.
- [34] William Hintzman, “On the existence of best analytic approximations”, *Journal of Approximation Theory* **14** (1975), 20–22.
- [35] K. Hoffman, *Banach spaces of analytic functions*, Prentice-Hall, 1962.
- [36] Stephan A. Ivanov, [1995] “Application of the planar model to the analysis and design of the Y-junction strip-line circulator”, *IEEE Transactions on Microwave Theory and Techniques* **43**:6 (1995).
- [37] Taisuke Iwai, S. Ohara, H. Yamada, Y. Yamaguchi, K. Imanishi, and K. Joshin, “High efficiency and high linearity InGaP/GaAs HBT power amplifiers: matching techniques of source and load impedance to improve phase distortion and linearity”, *IEEE Transactions on Electron Devices*, **45**:6 (1998).
- [38] V. E. Katsnelson and B. Kirstein, “On the theory of matrix-valued functions belonging to the Smirnov class”, in *Topics in Interpolation Theory*, edited by H. Dym, Birkhäuser, Basel, 1997.
- [39] Paul Koosis, *Introduction to  $H_p$  spaces*, Cambridge University Press, Cambridge, 1980.
- [40] Brian J. Markey, Dilip K. Paul, Rajender Razdan, Benjamin A. Pontano, and Niloy K. Dutta, “Impedance-matched optical link for C-band satellite applications”, *IEEE Transactions on Antennas and Propagation* **43**:9 (1995), 960–965.
- [41] Wen C. Masters, Second H-Infinity Program Review and Workshop, Office of Naval Research, 1999.
- [42] Z. Nehari, “On bounded bilinear forms”, *Annals of Mathematics*, **15**:1 (1957), 153–162.
- [43] Ruth Onn, Allan O. Steinhardt, and Adam W. Bojanczyk, “The hyperbolic singular value decomposition and applications”, *IEEE Transactions on Signal Processing*, **39**:7 (1991), 1575–1588.
- [44] David M. Pozar, *Microwave engineering*, third edition, Prentice-Hall, Upper Saddle River (NJ), 1998.
- [45] Vladimir V. Peller and Sergei R. Treil “Approximation by analytic matrix functions: the four block problem”, preprint, 1999.
- [46] Marvin Rosenblum and James Rovnyak, *Hardy classes and operator theory*, Oxford University Press, New York, 1985.
- [47] Walter Rudin, *Functional analysis*, McGraw-Hill, New York, 1973.
- [48] Walter Rudin, *Real and complex analysis*, McGraw-Hill, New York, 1974.
- [49] David F. Schwartz and J. C. Allen, “ $H^\infty$  approximation with point constraints applied to impedance estimation”, *Circuits, Systems, & Signal Processing* **16**:5 (1997), 507–522.

- [50] Abraham A. Ungar, “The hyperbolic Pythagorean theorem, in the Poincaré disk model of hyperbolic geometry”, *Amer. Math. Monthly* **108**:8 (1999), 759–763.
- [51] H. P. Westman, (editor), *Reference data for radio engineers*, 5th edition, Howard W. Sams, New York, 1970.
- [52] M. Ronald Wohlers, *Lumped and distributed passive networks*, Academic Press, New York, 1969.
- [53] Dante C. Youla, “A tutorial exposition of some key network-theoretic ideas underlying classical insertion-loss filter design”, *Proceedings of the IEEE* **59**:5 (1971), 760–799.
- [54] Dante C. Youla, F. Winter, S. U. Pillai, “A new study of the problem of compatible impedances”, *International Journal Circuit Theory and Applications* **25** (1997), 541–560.
- [55] Paul Young, *Electronic communication techniques*, 4th edition, Prentice-Hall, Upper Saddle River (NJ), 1999.
- [56] Nicholas Young, *An introduction to Hilbert space*, Cambridge University Press, Cambridge, 1988.
- [57] Eberhard Zeidler, *Nonlinear functional analysis and its applications*, vol. III, Springer, New York, 1985.
- [58] Kehe Zhu, *Operator theory in function spaces*, Dekker, New York, 1990.

JEFFERY C. ALLEN  
SPAWAR SYSTEM CENTER  
SAN DIEGO, CA 92152-5000

DENNIS M. HEALY, JR.  
DEPARTMENT OF MATHEMATICS  
UNIVERSITY OF MARYLAND  
COLLEGE PARK, MD 20742-4015  
UNITED STATES  
dhealy@math.umd.edu